Memoirs of Museum Victoria 74: 291–324 (2016) Published 2016

ISSN 1447-2546 (Print) 1447-2554 (On-line)
http://museumvictoria.com.au/about/books-and-journals/journals/memoirs-of-museum-victoria/

Description of new cranial material of *Propalorchestes* (Marsupialia: Palorchestidae) from the Middle Miocene Camfield Beds, Northern Territory, Australia

Peter W. Trusler[1,*] and Alana C. Sharp[2]

[1] School of Earth, Atmosphere and Environment, Monash University, Clayton, Victoria, 3800 Australia.
[2] School of Science and Technology, University of New England, Armidale, NSW, 2351 Australia.
* To whom correspondence should be addressed. E-mail: peter@petertrusler.com.au

Abstract

Trusler, P.W. and Sharp, A.C. 2016. Description of new cranial material of *Propalorchestes* (Marsupialia: Palorchestidae) from the Middle Miocene Camfield Beds, Northern Territory, Australia. *Memoirs of Museum Victoria* 74: 291–324.

Additional material referable to *Propalorchestes novaculacephalus* from the middle Miocene Camfield Beds is described. A cranium prepared in 1999-2000 from material collected on the T. H. Rich expedition of 1981 represents the most complete skull of the genus found to date. The detailed preservation of the previously unknown rostral anatomy supports the hypothesis that *Propalorchestes* possessed retracted nasal morphology. Cheek teeth from the skull and an additional isolated mandibular fragment from the same site, adds to the dental record for the genus. It further supports the intermediate condition of the molar morphology between the fully bilophodont *Palorchestes* and the subselenodont/semilophodont wynyardiid morphologies. The highly retracted nasal morphology and corresponding mandibular features demonstrate an advanced and highly derived condition in contrast to the plesiomorphic features previously described for the basicranium. In comparison to the generalized rostral anatomy of the sister group, the early to middle Miocene Diprotodontidae, this more complete record of *Propalorchestes* cranial morpholgy, suggests a significantly earlier origin for the highly derived facial anatomy in the Palorchestidae.

Keywords

Propalorchestes, Palorchestidae, Vombatomorphia, Vombatiformes, Marsupialia, Miocene, Camfield Beds, Bullock Creek Local Fauna.

Introduction

Museum Victoria and Monash University, under the instigation and direction of Dr. T. H. Rich, undertook a field collection survey of northern and central Australia between 26 May and 30 July 1981. Seven tons of predominantly limestone rock and nodules, containing bird, reptile and mammal skeletal material, was collected over a three-week period at Bullock Creek in the Northern Territory and immediately transported to Melbourne, Victoria. The rock was subsequently divided between Museum Victoria and the Queen Victoria Museum and Art Gallery, Launceston, Tasmania, to share the preparatory tasks. A substantial proportion of this material was prepared during the ensuing decade and a number of studies have been published on the dominant taxa from the site (Flannery et al., 1982; Smith and Plane, 1985; Murray et al., 1987, 2000a, 2000b; Murray, 1990; Murray and Vickers-Rich, 2003). A quantity of unprepared material remains in the collections of both institutions and it is hoped that this report of two exceptional specimens collected during the T. H. Rich 1981 Expedition, encourages further preparation and renewed examination of the Bullock Creek Local Fauna (LF). The excellent, uncrushed state of preservation of these specimens in limestone allows detailed description of external surfaces and internal morphology not usually possible with fossils from non-calcareous lithologies; the Carl Creek Limestone of the Riversleigh World Heritage Area (WHA) northwestern Queensland being a notable example (Archer et al., 1991; Wroe et al., 1998; Black and Hand, 2010; Black et al., 2010, 2012).

During prospecting at the Bullock Creek locality, a limestone-encased skull, QVM2000GFV459, was provisionally recognized as being different to the majority of zygomaturine (*Neohelos* spp.) material from the Camfield Beds at Bullock Creek. An extract from Rich's field diary entry of 10th July 1981 reads:

"Recovered five partial diprotodontid skulls today from Top Quarry. One of them has a steeply dipping forehead apparently as suggested of what little can be seen. If so, this may be a palorchestid with retracted nasals instead of *Neohelos*."

The first description of *Propalorchestes* cranial remains was presented by Murray (1986) from a single Bullock Creek specimen. Subsequently prepared material from the same site and from the Riversleigh World Heritage Area (Black, 1997a,

b) extended that information to form a total collection of eight specimens representing eight individuals: three dentary fragments, a maxilla, a neurocranial fragment and three isolated teeth. Despite this paucity of material, a second species of *Propalorchestes* was described by Murray (1990) from the Riversleigh WHA Faunal Zone A and B deposits. In doing so, Murray (1990) contributed substantial insights, not only with respect to the origins and trends in diversification of the Vombatomorphia throughout the Miocene, but also by demonstrating the early divergence and distinction of the palorchestid lineage. Since that time, Black (2006) has published data on a further four *Propalorchestes* specimens, (another maxillary fragment and three isolated teeth from the Riversleigh WHA deposits), to re-appraise the dental morphology and re-assign specimens within the genus. This material has been further reassessed by Arena et al. (2015) with reassignments of *Pr. ponticulus* specimens to *Pr. novaculacephalus*, and the inclusion of new material from each species. In addition, several new species of *Palorchestes* have been described since 1990: 1) a moderately large M^1 as *P. selestiae* Mackness, 1995, from the Bluff Downs Local Fauna; 2) A small M^1 as *P. anulus* Black, 1997a, from the Riversleigh WHA, Queensland, Faunal Zone D deposits; and 3) *P. pickeringi* Piper, 2006, another small form based on a collection of dental material, maxillary fragments and a mandible fragment from the Nelson Bay LF of Victoria. Piper's description of the early Pleistocene *P. pickeringi,* allowed the identification of an isolated *Palorchestes* M_3 reported from the Pliocene Hamilton LF by Turnbull & Lundelius (1970) and suggested that further material from that site and the Pliocene Curramulka LF (Pledge, 1991) be re-examined in that regard (Piper, 2006; Lundelius, this volume). There also remains a significant number of isolated dental specimens and fragmentary material in collections from a range of late Miocene to Pleistocene sites in South Australia, Victoria and Queensland that exhibit intermediate morphologies or have proven difficult to diagnose (Pledge 1991, 1992: Price and Hocknull, 2005; Piper, 2006; Shean, 2007; Lundelius, this volume). In all, this suggests that multiple palorchestid forms ranged throughout the Miocene to Pleistocene and indicates that a niche for smaller species remained within the trend to gigantism into the early Pleistocene. These studies based primarily on dental material, continue to cast doubt on the linear evolution of the group that had seemed apparent from the three previously known *Palorchestes* species: *P. painei, P. parvus* and *P. azael* (Murray, 1990; Pledge 1991, 1992; Mackness 1995; Black 1997, 2006; Piper, 2006; Price and Hocknull, 2005; Shean, 2007; Lundelius, this volume).

An appreciation of the unusual cranial morphology of the group has been wanting for a century, and yet, the first palorchestid material to be discovered was a rostral fragment of *Palorchestes azael* from Victoria in 1851 (Owen, 1873). Although it was perplexing in several respects, Owen (1876) ascribed an affinity between *Palorchestes* and the Macropodidae on the basis of his assessment of gross dental morphology and lower jaw proportions from new mandibular material from Wellington Caves, N.S.W. De Vis (1883) echoed those sentiments when describing a juvenile *P. azael* mandible from St Ruth, Darling Downs, Queensland. He described a second species, *P. parvus,* from a fragmentary skull comprising maxilla, mandible and rostral elements, but reiterated the macropod affinity on the basis of dental morphology (De Vis, 1895). The relationship between *Palorchestes* and Macropodidae continued to be consolidated by a succession of authors until Woods (1958) redefined *Palorchestes* and demonstrated a closer relationship with the Diprotodontidae (Mackness, 1995, 2008). In so doing, Woods (1958) drew attention to the unusual rostral anatomy in both *P. azael* and *P. parvus,* but did not include rostral features in his diagnoses. Woodburne (1967) described a third species *P. painei* on the basis of poorly preserved cranial and mandibular material from the late Miocene Alcoota LF. By 1974, more complete and better preserved *P. painei* skulls from that locality informed understanding of the cranial anatomy of the Palorchestidae, but detailed studies of the newer *P. painei* material have not been published (Murray, in prep).

Tate (1948) erected the Palorchestinae as a subfamily within the Macropodidae, but it was subsequently relocated within the Diprotodontidae by Stirton (1967), and revised to its own family, Palorchestidae, by Archer and Bartholomai (1978) on the basis of the growing list of distinctive cranial and postcranial characters evidenced in new specimens (Mackness 2008). It is not unsurprising that the morphological variation and function of cranial structures within the family remain enigmatic, given only *P. painei* has been described from relatively complete skull specimens.

The description herein of two uncrushed and well-prepared specimens of an early palorchestid from the Queen Victoria Museum and Art Gallery paleontology collections provides, in combination with the work of Murray (1986, 1990), Black (1997a-b, 2006) and Arena et al., (2015), a significant insight into the cranial, mandibular and dental morphology of the family during the Miocene. Furthermore, this description adds to our knowledge of the unique rostral anatomy of the earliest known palorchestid genus. Together with *Palorchestes painei*, this becomes only the second species in the Palorchestidae described with this degree of completeness.

Abbreviations

Institutional abbreviations – AM, Australian Museum, Sydney; AMF, fossil collection of the Australian Museum; AR, temporary paleontological collection of the University of New South Wales, Sydney; CPC, Commonwealth Paleontological Collection, Canberra; MV, Museum Victoria, Melbourne; NMV P, Museum Victoria Paleontology Collection Melbourne; NTMP, paleontological collection of the Northern Territory Museum, Darwin; QMF, fossil collection of the Queensland Museum, Brisbane; QVMAG, Queen Victoria Museum and Art Gallery, Launceston, Tasmania; QVM-GFV, paleontological collection of the Queen Victoria Museum and Art Gallery, Launceston; SAM, South Australian Museum, Adelaide; SAMP, paleontological collection of the South Australian Museum; SGM, Spencer and Gillen Museum (Northern Territory Museum, Alice Springs); UCMP, University of California Museum of Paleontology, Berkeley.

Other abbreviations – LF, Local Fauna; Ma, million years; WHA, World Heritage Area; FZ, Faunal Zone.

Camfield Beds fossil site name abbreviations – Top, "Top Quarry" – site designation WV 113, Wave Hill 1:250,000 Geological Map series, sheet SE 52-08, 2nd Ed, 2003, (noted to be topographically higher than the other sites and rich in dromornithid bird material); HC, "Horseshoe Central" (site designation VW 123); HW site, "Horseshoe West" (200 m west of HC).

Dental abbreviations – Molar number homology is that proposed by Luckett (1993). I^n, upper incisor; I_n, lower incisor; M^n, upper molar; M_n, lower molar; P^n, upper premolar; P_n, lower premolar.

Generic abbreviations – Because the two Palorchestidae genera discussed throughout this paper begin with '*P*', the following generic abbreviations are used: *P.* = *Palorchestes*; *Pr.* = *Propalorchestes.*

Geographic, Geologic and Paleoecological Setting

The Camfield Beds outcrop along the Bullock Creek and Cattle Creek tributaries of the Camfield River at latitude 17°–17.5° S – Longitude 131.5° E (Randal and Brown, 1967; Plane and Gatehouse,1968). (fig. 1). They consist of light-coloured calcareous siltstone, sandy siltstones to silty sandstones, conglomeratic limestone, calcimudstone, chalcedonic limestone and gypsiferous siltstone (Murray, 1986; Murray et al., 2000a, b). The complex, somewhat chaotic deposits are essentially palaeovalley fills where vertebrate fossils are concentrated in limestone facies. Murray (1986) described the facies as typically ferruginized at their bases and silicified towards the top. Murray and Megirian (1992) interpreted the deposits to be formed by fluviatile channels and associated billabongs. Randal and Brown (1967) originally postulated a normally saline lacustrine, lagoonal or estuarine environment of deposition, occasionally flooded by freshwater inflows.

The late Oligocene and Miocene across northern Australia is characterized by carbonate deposition events (Megirian et al., 2004). In the case of the Carl Creek Limestone deposition (Riversleigh WHA), McGowran and Li (1994) attributed this to the global marine Miocene Oscillation events of climatic reversals (and the accompanying sea level changes) within the general trend to cooling (Megirian et al., 2004). Faunal composition comparisons between the Bullock Creek and Alcoota sites also lead Murray and Megirian (1992) to suggest the Bullock Creek habitat was characteristically open woodland to savanna with seasonal and and/or cyclical climate fluctuations showing severe periods of drought and a trend to increasing aridity over time. The late Oligocene to late Miocene transitions at Riversleigh are interpreted to have variously involved forested habitats throughout: specifically that FZ A represents open forests and that rainforest developed through FZ B to FZ C during the early and middle Miocene, only to return to an open forest habitat by FZ D (represented by the Encore LF) in the late Miocene (Travouillon et al., 2009). The likelihood that riparian forests variously provided additional faunal components to the records from the localities and some site-specific taphonomic biases (particularly in regards to individual cave accumulations), have doubtlessly complicated the interpretation of the respective wider ecosystems (Murray and Megirian, 1992; Megirian et al., 2004; Travouillon et al., 2009).

Until recently, detailed age constraints for the LF's within the northern Australian limestone deposits from this interval have been generally lacking (Megirian et al., 2010). Marsupial biochronology has been the main means of correlating between sedimentary basins (Stirton et al., 1967, 1968; Woodburne et al., 1985, 1994; Rich, 1991; Megirian, 1994, 1997; Black, 1997b, 2010; Archer et al., 1997; Meyers & Archer 1997; Megirian et al., 2010; Murray et al., 2000a-b). For example, morphoclines of key taxa such as *Neohelos*, have proven critical in interpreting the stratigraphic relationship between localities and the sites within them (Black et al., 2013). Bullock Creek *Wakaleo vanderleueri* material described by Murray and Megirian (1990) shows fewer differences from *W. oldfieldi* than previously thought by Clemens & Plane (1974) when they originally described these thylacoeonids from the Camfield Beds and Wipajiri Formation respectively (Gillespie et al., 2014). This suggested that the age of the Bullock Creek LF is closer to that of the early Miocene Kutjamarpu LF than to that of the Alcoota LF (Murray & Megirian, 1992), but Travouillon *et al., (*2006) concluded that the biostratigraphic position of the Kutjamarpu LF remained ambiguous. Greater agreement has been found for the correlation of the Riversleigh Faunal Zone A deposits to those of the late Oligocene Ngama LF (Archer et al., 1997; Murray and Megirian 2000; Myers and Archer, 1997; Woodburne et al., 1994) and the Ngapakaldi LF, both from the Etadunna Formation, South Australia (Black, 1997b, 2010; Meyers and Archer, 1997) and these in turn, share six taxa (Travouillon et al., 2006).

In a detailed comparison of Bullock Creek and Alcoota sites, Murray & Megirian (1992) concluded that the LF's from each site demonstrate a later Miocene age for Alcoota and that Bullock Creek represents an earlier stage of the same evolutionary succession with an estimated 3 Ma interval between the localities. *Wakaleo vanderleueri* is also represented in FZ D from Riversleigh (Arena et al., 2014) together with the only record of *Palorchestes anulus* (Black, 1997a). The larger *Palorchestes painei* (Woodburne, 1967) appears at Alcoota and represents a more advanced stage of evolution to the other Miocene palorchestids (Murray and Megirian, 1992). These occurrences might suggest some correlation between Bullock Creek and Riversleigh's FZ D, but that other material within FZ D was deposited later, during the time interval between Bullock Creek and Alcoota deposits.

Strong faunal correlations exist between Riversleigh's Faunal Zone C deposits and the Northern Territory's Bullock Creek LF through sharing *Nimbadon*, *Nimbacinus, Neohelos and Propalorchestes* species (Black, K., 1997b, 2010; Myers and Archer, 1997; Megirian et al., 2004; Travouillon et al., 2006, 2009; Arena et al., 2014). The stage of evolution studies of *Propalorchestes* are therefore significant to that comparison (Black et al., 2012; Arena et al., 2015)

Woodhead et al. (2015) have presented radiometric U–Pb dates on speleothem for the Riversleigh WHA that span a time

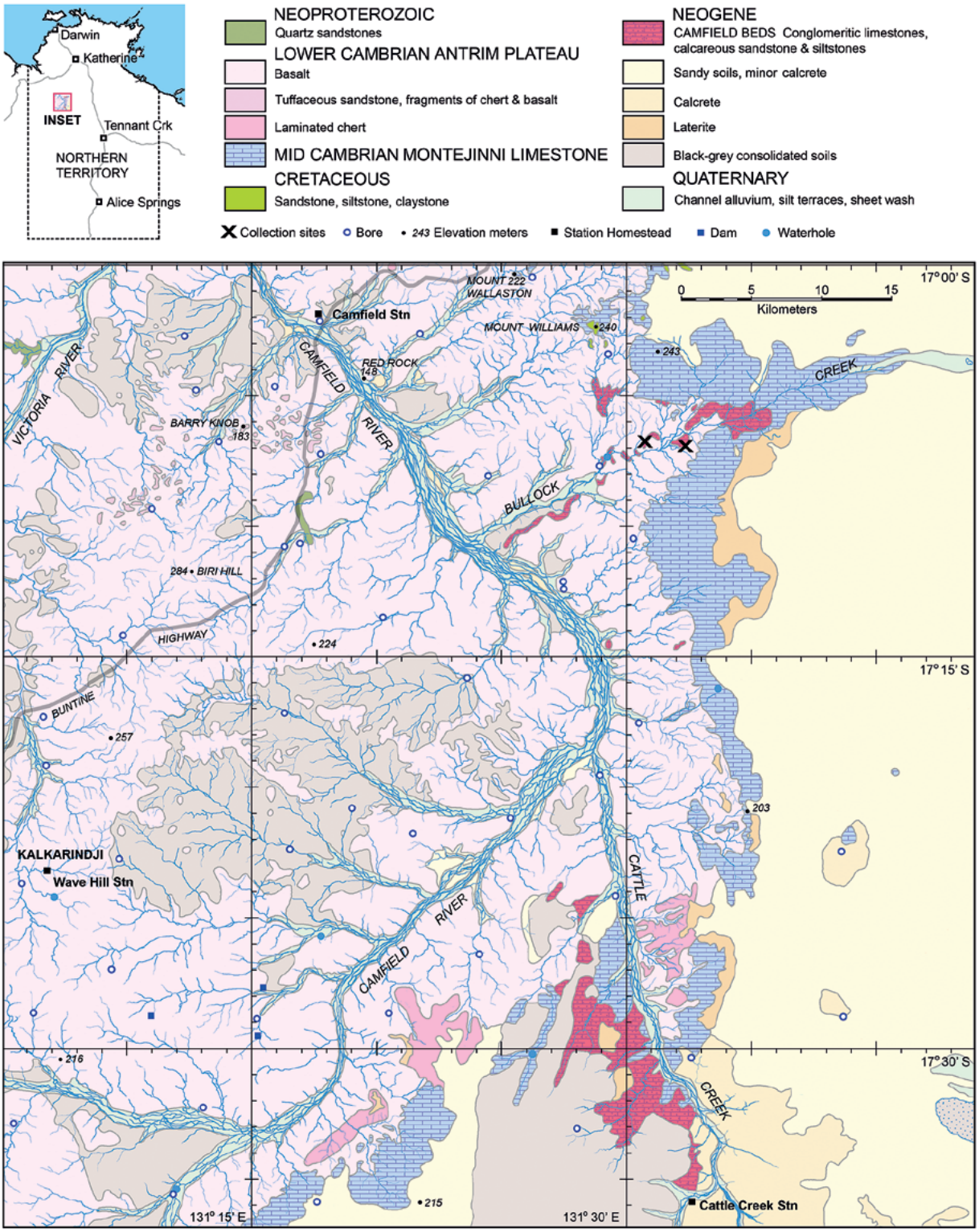

Figure 1. Bullock Creek regional geologic map showing the early to middle Miocene Camfield Beds and their relationship to Cambrian limestones and Neogene to recent drainage systems. Abridged from Wave Hill 1:250,000 Geological Map series, sheet SE 52-08, 2nd Ed, 2003. For fossil site details refer to Murray & Megirian (1992) and files held at the Northern Territory Museum.

interval of ~5–6 Ma between the oldest and youngest Miocene deposits: Neville's Garden at 18.24 ± 0.29 Ma and Whitehall at 13.48 ± 0.45 Ma, respectively. These effectively bracket the early Miocene (18.2–16.5 Ma) and middle Miocene (15.1–13.5 Ma) deposits that represent the upper part of Faunal Zone B and most of Faunal Zone C from Riversleigh. The extensive biostratigraphic studies of the fauna within the Riversleigh deposits corroborate a middle Miocene age for the Bullock Creek LF (Arena, 2004; Woodhead et al., 2015). While Murray and Megirian (1992) suggested that Bullock Creek might be transitional Bairnsdalian-Mitchellian, a depositional period within the Bairnsdalian stage (15.0–10.5 Ma) is more parsimonius.

The skull QVM2000GFV459 was collected from an area previously prospected and systematically excavated by M. D. Plane and associates of the Bureau of Mineral Resources (Murray and Megirian, 1992) at a site informally known as 'Top Quarry' (Top). The mandibular fragment was subsequently revealed, also at QVMAG, through preparation of limestone rock excavated at the same site during the T. H. Rich 1981 Expedition. Murray and Megirian (1992) suggested Top represented point bar accumulations or low energy fluvio-lacustrine deposits in which minimal transport and dissociation has occurred. They regarded the complex Bullock Creek sites to represent sequential, but intermittent, accumulations over a geomorphologically significant period of time.

Materials and Methods

Much of the excavation work at Top was achieved using plug-and-feather techniques. QVM2000GFV459 and QVM2000GFV406 were acetic acid etched and a log of the preparation is kept at QVMAG. Measurements from all specimens were taken using Sontax 0–150 mm Digital Callipers and mechanical dividers/callipers.

QVM2000GFV459 and QVM2000GFV406 where scanned using computed tomography (CT) with a Siemens Somaton Defintion Edge (Siemens Medical Solutions) at Launceston General Hospital. The specimens were scanned at 0.75 mm slice thickness and 0.5 mm interslice distance to produce 629 slices for QVM2000GFV459 and 373 slices for QVM2000GFV406. CT data for QVM2000GFV459 were imported and processed in Avizo 7.0 (Visage Imaging, Inc.) to produce three-dimensional (3D) reconstructions of the cranium, endocranial sinuses and brain cavity. Automatic and manual segmentation (the process of isolating and selecting structures based on their grey values, or density) was performed to isolate each structure and produce 3D surface reconstructions. To produce a 3D PDF model, the surface reconstructions were simplified and exported as Wavefront (*.obj) generic 3D files, imported to Adobe 3D Reviewer (available in Adobe Acrobat 9 Pro Extended) and converted to a single Universal 3D (*.u3d) file. The U3D file was then embedded in the PDF document using Adobe Acrobat 9 Pro and can be viewed in Adobe Reader.

The preparation of the reconstructed line illustrations for *Propalorchestes* are based on measurements of QVM2000GFV459 and QVM2000GFV406 and not photographic or camera lucida tracings. All diagrams were prepared digitally. Graphic measurement processes include a margin of error. This was held within acceptable limits and checked against the CT scan data. It has allowed for minor deformations of the cranium to be estimated. Some asymmetry in the original skull was present in life and can clearly be seen in the disparity between bilateral suture lines. Where detected, this has been retained. Distortions introduced through taphonomic influences may have acted in slightly independent ways on the specimen. (see Preservation.) Factors such as torsion were minor, and retro-deformation of the cranial outline has been undertaken to correct these artefacts. That process is more subjective and it is hoped that the methodology to include line art, circumvents the parallax inherent in photography and has improved accuracy of presentation in excess of any margin of error in estimating and correcting deformations.

Higher-level systematic nomenclature follows Aplin and Archer (1987). Craniomandibular terminology follows Stirton (1967), Murray (1986) and Murray et al. (2000a, b). The dental nomenclature for *Propalorchestes* follows Rich and Archer (1979) and Murray (1990). Dental notation follows Luckett (1993).

Systematic palaeontology

Marsupialia Illiger, 1811

Diprotodontia Owen, 1866

Vombatiformes Woodburne, 1984

Vombatomorphia Aplin and Archer, 1987

Palorchestidae Tate, 1948; Archer and Bartholomai, 1978

Propalorchestes Murray, 1986

Type species. ***Propalorchestes novaculacephalus*** Murray, 1986
Additional species. ***Propalorchestes ponticulus*** Murray, 1990

Diagnosis. Refer to the original diagnosis of Murray (1986) and additions of Murray (1990) and Black (2006).

Remarks - Propalorchestes novaculacephalus has the smallest known palorchestid skull with the possible exception of *Pr. ponticulus* that is presently only described from smaller isolated dental material and mandibular fragments. The new, small mandibular material referred herein to *Pr. cf novaculacephalus*, indicates the sizes of *Propalorchestes* forms overlapped considerably (tables 3–4, figs. 14C, D, 15C). The M^1 of *Palorchestes anulus* is only slightly larger than the *Propalorchestes* material and skull dimensions for *P. annulus* would also likely overlap those of *Pr. novaculacephalus*.

Propalorchestes novaculacephalus **Murray, 1986, pp. 195–211, figs. 1–6: Murray 1990, pp. 39–51, figs 1-3: Black, 2006, pp. 351–361, figs. 1–2.**

Holotype. NTM P8552-10: left and partial right side of neurocranium including most of the zygomatic arch and latex endocast.

Type locality. "Top Site" quarry in the Camfield Beds, Bullock Creek tributary of Camfield River, north central Northern Territory (Plane and Gatehouse 1968; Murray, 1986).

Distribution and Age. Bullock Creek LF, Camfield Beds, Northern Territory middle Miocene (Woodbume et al., 1985), Riversleigh WHA Faunal Zone B–C, middle Miocene (Black, 2006; Travouillon et al., 2006; Woodhead et al., 2015; Arena et al., 2015).

Paratypes. NTM P862-27, right maxilla with M^{1-2}, Bullock Creek LF; NMVP 187282, right dentary with M^{2-4}, HW site, Bullock Creek LF, Camfield Beds, Northern Territory (Murray, 1990)

Referred material. QMF12429, isolated right M^2, Henk's Hollow LF, Riversleigh, northwestern Queensland (Archer et al., 1989, 1991); QMF50605, left maxilla with dP^3, P^3, M^{1-3}, Jim's Carousel LF; QMF51399, left M^1, Henk's Hollow LF; QMF30883, right partial maxilla with P^3, M^1 (broken), Wayne's Wok LF; and QMF30884, right M^1, Camel Sputum LF (Black, 2006); QMF537310, Cadbury's Kingdom LF (Arena et al., 2015).

Additional material described herein. QMV2000GFV459, near complete cranium with right M^{1-4}, left P^3, M^{1-4}, M^{2-4} crowns sheared off, Top site, Bullock Creek LF, Camfield Beds, Northern Territory; NMVP179093 isolated M^4 fragment, posterior moiety of crown, Top site, Bullock Creek LF; NMVP249851 isolated P^3 fragment, lingual half of crown, Horseshoe West Site, Bullock Creek LF; QVM2000GFV406, right dentary fragment with M_{2-4}, Top site, Bullock Creek LF.

Description

Preservation. QVM200GFV459, near-complete splanchnocranium with partial neurocranium: missing tip of nasal, ventral extremities of masseteric processes, mid region of the left zygomatic arch, pterygoid wings, (incl. rim of choana), nuchal plate, most of basicranium, mastoid processes, paraoccipital processes, associated auditory osteology and occipital condyles. All incisors, except the right I^1 root and crown base, are lost. Cheek teeth well worn, highly fractured with considerable crown enamel losses; right M^{2-4} crowns sheared off, left P^3 missing.

Cranial overview. The preservation and preparation of the external surface is excellent for the most part. Some of the suture lines and damaged occipital morphology are slightly over-etched. Much of the internal structure of the skull is evident including the thin septa between sinuses and residual parts of the bony nasal septum, nasal conchae and cribiform plate. Some limestone matrix remains supporting this delicate osseous anatomy and occupies fully enclosed sinuses. The neurocranium is rotated 2° to the right with respect to the splanchnocranium. The slight torsion of the skull, (about the narrow mid-region), probably results from the loss of the left zygomatic arch and fracture of the right arch. The basicranium has been sheared-off, abraded and the bone weathered, indicating that this aspect of the skull had been exposed for some time either prior to complete burial or through subsequent weathering of the limestone rock.

In dorsal view, the skull form is narrowly waisted dividing an ovoid, (approx. 90 mm long, 65 mm wide) crested neurocranium from a wedge-shaped splanchnocranium. From the "waist," the central region of the skull broadens anteriorly to form a trapezoidal prism, (approx. 72 mm long, 72 mm wide at the frontal). The anteriorly facing surface of this prism connects perpendicularly with the anterior roots of the zygoma to form a transverse, flat facial plane with small, forwardly directed orbits. A narrow rostrum, approximately half the width of the facial plane, projects abruptly from this transverse surface. The entire dorsal rostral surface is excavated forming a 100 mm long, nasal cavity; widest sub-proximally, 45 mm from the facial plane, where it forms a heart-shaped aperture (figs. 2A, 3A).

In anterior view, the dorsal skull outline is strongly crested with broadly convex frontals separated by the shallow frontal depression. The orbits are positioned well below the level of the nasals, within the dorsal one third of the facial surface. The infraorbital foramina are prominent and the wide proximal part of the nasal aperture is oval-shaped in this view (figs. 4A, 5A).

In lateral view, the dome of the neurocranium is accentuated by the sagittal crest and the rostrum (approx. 123 mm long from the orbital rim), deflected 24° below the plane of the cheekteeth (figs. 4B, 5B).

Although broken at the free rostral nasal process, the sutured portion of the nasals are short and highly retracted. The lateral maxilla-premaxilla walls are highly excavated with the premaxilla ascending processes surmounting their entire extent. The anterior portion of the nasal cavity is a narrow slot defined by thinly crested lateral premaxilla walls. A strong premaxilla midline eminence surmounts a shallowly concave, but rounded rostral tip. The incisor alveolar arcade is arcuate. The rostral diastema is flat and gently re-curved, with sharp diastemal crests and well-defined sulci on each side of the ventral midline. The sulci are deepest where they accommodate incisive foramina and continue posteriorly for two thirds of the external palate. The maxilla tooth rows are proportionately small for the size of the skull, flat in the frontal plane, straight and parasagittal. The zygomatic arch is deep, but proportionately thin; the lateral surface of the jugal portion is concave, curves gently downwards to the masseteric process while maintaining a vertical orientation and is defined by a dorsal crest along the jugal. The crest becomes anteriorly directed at the masseteric process; the masseteric jugal crest would have delimited the dorsal and anterior extent of the *m. masseter superficialis*. The zygomatic process of the squamosal also projects perpendicularly, to form the squamosal sulcus and concave posterior floor of the temporal fossa. The posterolateral edge of the temporal fossa is angled approximately 125° to the midline before flattening to form the lambdoid crests. These crests form a distinctive arc that projects over, and restricts, the small occipital plate. The posterior face of the occiput is deeply excavated and though concave, slopes posteriorly at approximately 125° from the cheektooth plane for the part that has been preserved. The postglenoid fossa is clearly defined posteriorly by an extensive, but thin ventral crest that curves anterolaterally. The jugal contributes a slight curvature that provides lateral confinement

Table 1. Cranial dimensions for *Propalorchestes novaculacephalus*; asterisk denotes data from NTMP862-27; measurements in mm.

Specimen **Data source**	**NTM8552-10 Holotype** **Murray 1986**	**QVM2000GFV459** **Trusler & Sharp**
Locality/site	Bullock Creek/Top	Bullock Creek/Top
Max length	-	271.50
Rostral width @ max-premax suture	-	33.99
Inter-masseteric process inclusive width	-	121.78
Maxilla width @ M^1	-	62.65
Tooth row max. inclusive width @ M^1	-	59.79
Palatal width at M^1	-	35.03
Tooth row length P^3-M^4 left	-	77.76
Tooth row length P^3-M^4 right (estimate)	-	77.07
Molar row length M^{1-4} right	-	66.25
Rostral tip length Incisive foramen to premaxilla tip	-	58.91
Frontal process width (above orbits)	-	72.46
Cranial 'waist' width minimum	28.0	35.11
Bizygomatic width maximum @ glenoid region	166.4 (midline to left side x2)	143.40 (midline to right side x2)
Width lateral zygoma to 'waist' of cranium left	-	89.80
Temporal fossa width max. @ 'waist' right	55.0	49.99
Nasal cavity internal width max.	-	44.95
Subnasal crest length right	-	24.3
Subnasal crest length left	-	25.12
Subnasal crest width apart max. approx.	-	11.50
Subnasal crest width min apart approx.	-	9.25
Neurocranial length anterodorsal lacrimal suture to squamosal occiput wall	152.30	-
Cranial width at squamosal, immediately anterior to glenoid fossa	166.4	-
Cranial height	94.5	-
Occiput height condylar remnant - supraoccipital	69.3	-
Infraorbital foramen max diameter left	-	5.92
Infraorbital foramen max diam right NTMP862-27	10.0*	6.02
Infraorbital foramen min diameter left	-	5.04
Infraorbital foramen min diam right NTMP862-27	8.0*	5.76
Molar row length M^{1-4} left	-	-
Interorbital width	28.0	-
Temporal fossa width	55.0	-
Postorbital constriction minimum	28.0	-
Jugal & squamosal width @25 mm ant. to jugal border of glenoid fossa	37.0	Right 45.36 Left 48.08
Glenoid fossa length transverse	42.0	Right 40.74 Left 41.44
Glenoid fossa width sagittal	23.5	Right 10.19 Left 8.26
Sagital crest width	3.0 – 6.0	7.89
Sagital crest height	4.0 – 8.0	7.31

Table 2. Comparisons of cranial measurements between *Propalorchestes novaculacephalus* and QVM2000GFC459 expressed as percentages.

Measured feature	**QMV/*Pr. novaculacephalus***	***Pr. novaculacephalus*/QMV**
Bizygomatic width	90.01%	111.03%
Temporal fossa width	90.89%	110.02%
Sagittal crest height @ frontal-parietal suture	91.67%	109.09%
Infraorbital foramen maximum diameter	59.7%	167.5%
Infraorbital foramen minimum diameter	67.5%	148.1%

of the glenoid articular surface. There is a sharp medial limit to the glenoid, but most of this feature is not preserved. The remainder of the basicranial surface-features are not preserved (figs. 2–6, supplementary 3D interactive pdf).

Supraorbital region and Splanchnocranium. The approximately 5.5 mm high sagittal crest gradually decreases in sharpness anteriorly and diverges to form frontal crests at the parietal-frontal suture to a maximum angle of 30° either side of the midline. The frontal crests are well rounded: form a V-shaped crease at their median edge along the dorsal surface of the frontal to define the posterior edge of the frontal depression, and a gentle ridge along each posterolateral edge that probably delimited the anterior extent of the *m. temporalis.* The postorbital process of the frontal is weak and ill-defined. The frontal crests broaden and weaken anteriorly, but form the frontal eminence as a gently rounded boss over each orbit.

The frontal eminence curves downwards to contribute to the supraorbital region by a complex suture with the lacrimal to form a moderately rugose, frontolacrimal tuberosity. The frontal contributes the largest proportion to the structure; thus the lacrimal does not form an independent "lacrimal tuberosity." The frontolacrimal tuberosity continues the curving form of the frontal eminence. Each tuberosity contains two irregular pits at the dorsolateral extremity, but damage from acid-etching appears to have exaggerated the pitted texture. A dorsally directed groove extends from the left lacrimal foramen on the medial orbital wall. At the corresponding region of the right medial orbital wall, the form of the right lacrimal foramen is obscured by matrix residue, but is possibly represented by two small apertures. The lacrimal contributes only a small amount to the vertical facial plane at its dorsal extent. Its anterior edge sutures with the maxilla along the medial orbital rim before uniting with the jugal near the ventral border of the orbit and curving posteriorly down its internal surface. Posteriorly, the lacrimal-frontal suture runs vertically down the lateral cranial wall from the frontolacrimal tuberosity.

The nasal-frontal suture diverges at 45° from the midline on the dorsal surface of the skull and assumes the anterior edge of the frontal eminences at their anterolateral extent. At this point the nasals form a small lateral process to narrowly contact the maxilla ascending process that in turn, precludes nasal contact with the lacrimal. The nasal suture then turns medially to contact the flared dorsal extent of the premaxilla ascending process and traverses anteriorly before turning posteroventrally to continue along the internal roof of the nasal cavity. The nasal-premaxilla suture forms a slightly rugose, flattened ridge to the retracted dorsal rim of the nasal aperture at either side of the nasal spine, but is separated from the spine by a smooth, shallow parasagittal groove or narial notch (Woodburne, 1967). The narial notch is analogous to the nasal incisure seen in *Tapirus,* but the groove does not extend to form a sulcus (diverticular meatus) on the dorsal surface of the nasals (Boas & Paulli, 1908, 1924; Witmer *et al*., 1999).

Unfortunately, the rostral process of the nasal in QVM2000GFV459 has been fractured and lost, leaving little indication of its extent or morphology. The nasal process was narrow at its base; approximately one third of the maximum width of the nasal bones and one half the width of the anterior nasal roof. It may have formed a "nasal spine" with a weakly arched transverse profile at its base. It cannot be ascertained if this continued as a curved spine when seen in lateral profile, as in *Palorchestes painei* (Woodburne, 1967; Murray, pers. comm.) or as a flattened shelf with a small terminal spike as in *P. azael* (Trusler, in prep.). The former seems more likely in *Propalorchestes* and has been suggested by dotted outline in figures 3A, 5B.

The term "nasal spine" has been strictly applied here to the morphology of the nasal bone. This term is often used for the vertical midline projection of the premaxilla at the anterior of the nasal cavity. We have preferred the term premaxilla midline eminence for this feature, as suggested by Murray (pers. comm.), because it relates functionally to similar eminences or midline crests formed by the premaxilla or maxilla in other taxa with retracted nasal anatomy (see description p.6). Both features are common in taxa with retracted nasals or laterally excavated premaxilla and maxilla nasal walls. The nasal spine and premaxilla midline eminence both act as extended structural support for the free portion of the cartilaginous nasal septum at its dorsal and anteroventral extents respectively (Witmer et al., 1999).

An inverted trapezoid suborbital fossa (approx. 32.25 mm in height) is formed between the masseteric crest along the anterolateral edge of the jugal, the ventral orbital rim, and a vertical ridge formed by the maxilla-jugal suture line of the face; approximately 6.25 mm lateral to the infraorbital foramen. The fossa is smooth and shallowly concave. The maxilla-jugal suture then deflects laterally to join the lowest part of the jugal masseteric crest. This junction forms a sharp U-shape above the ventral edge of the maxilla root of the zygoma. This slightly concave region forms the dorsal extent of the subzygomatic sulcus that re-curves ventrally. The tip of each masseteric process is abraded to a point just dorsal to the

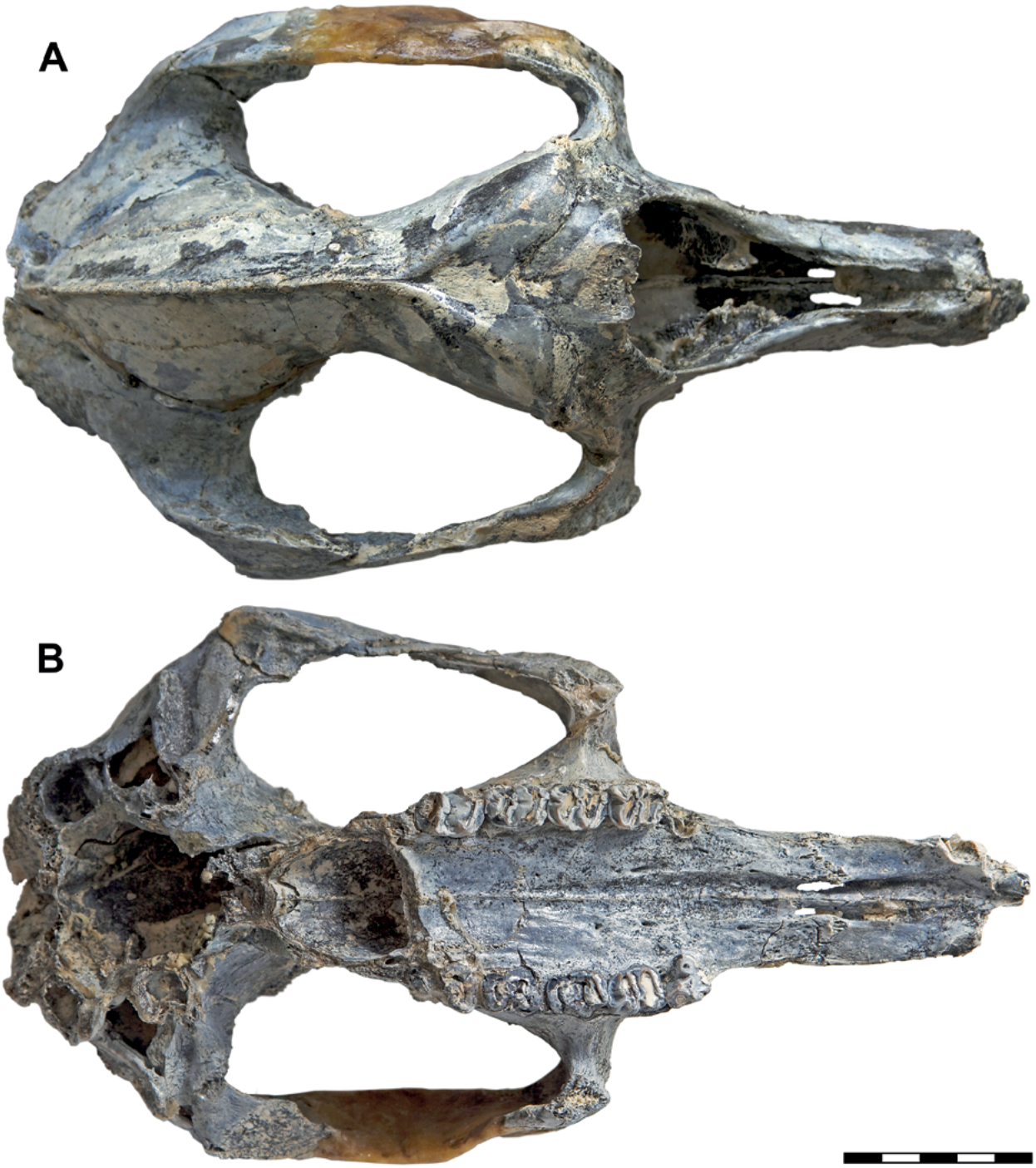

Figure 2. *Propalorchetes novaculacephalus* QVM2000GFV459: a, dorsal: b, ventral views of cranium, (not corrected for parallax); scale bar represents 5 cm.

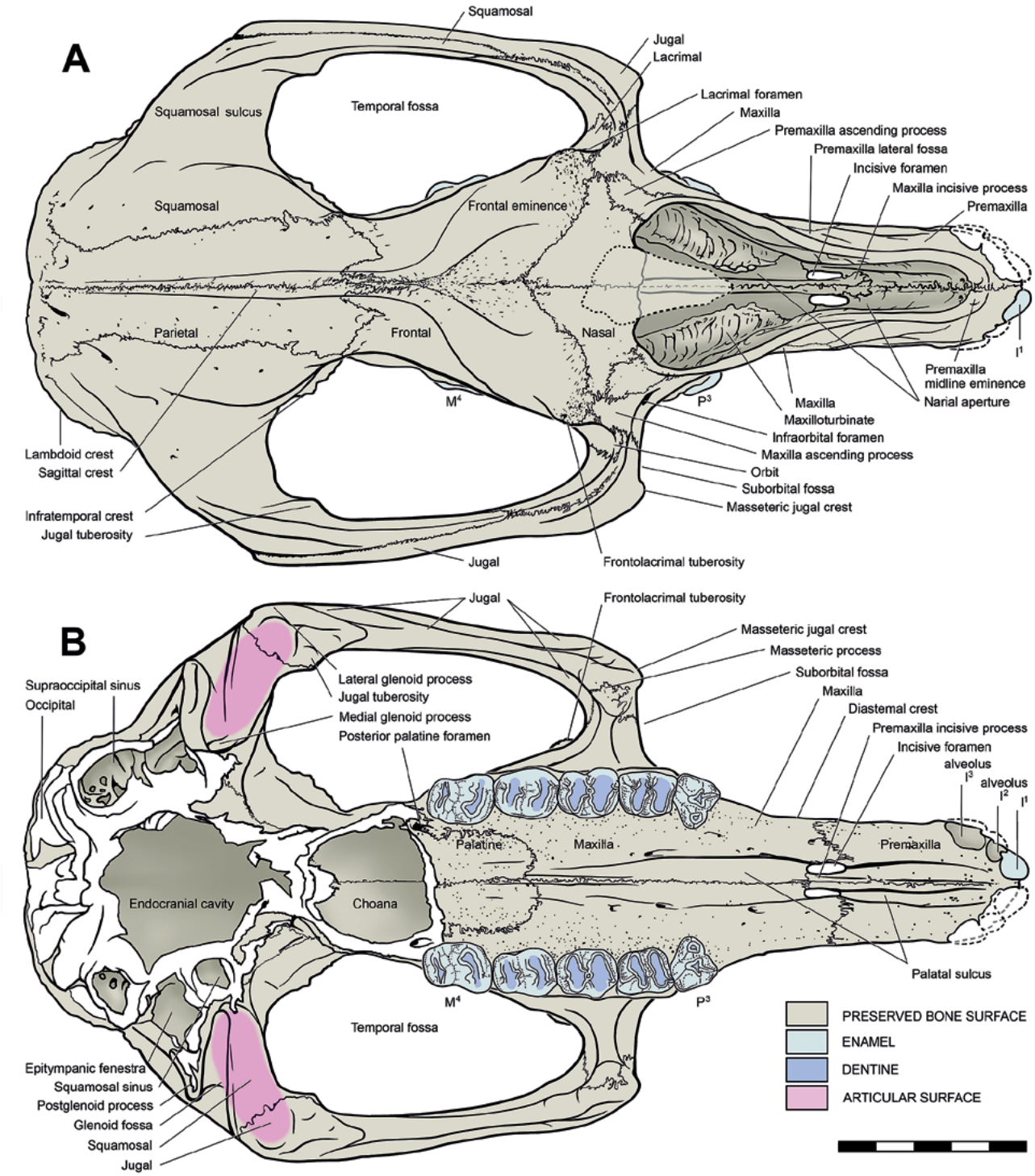

Figure 3. *Propalorchetes novaculacephalus* measured cranium outline diagram based on QVM2000GFV459: a, dorsal: b, ventral views of cranium; scale bar represents 5 cm.

Figure 4. *Propalorchetes novaculacephalus* QVM2000GFV459: a, anterior: b, lateral views of cranium, (not corrected for parallax); scale bar represents 5 cm.

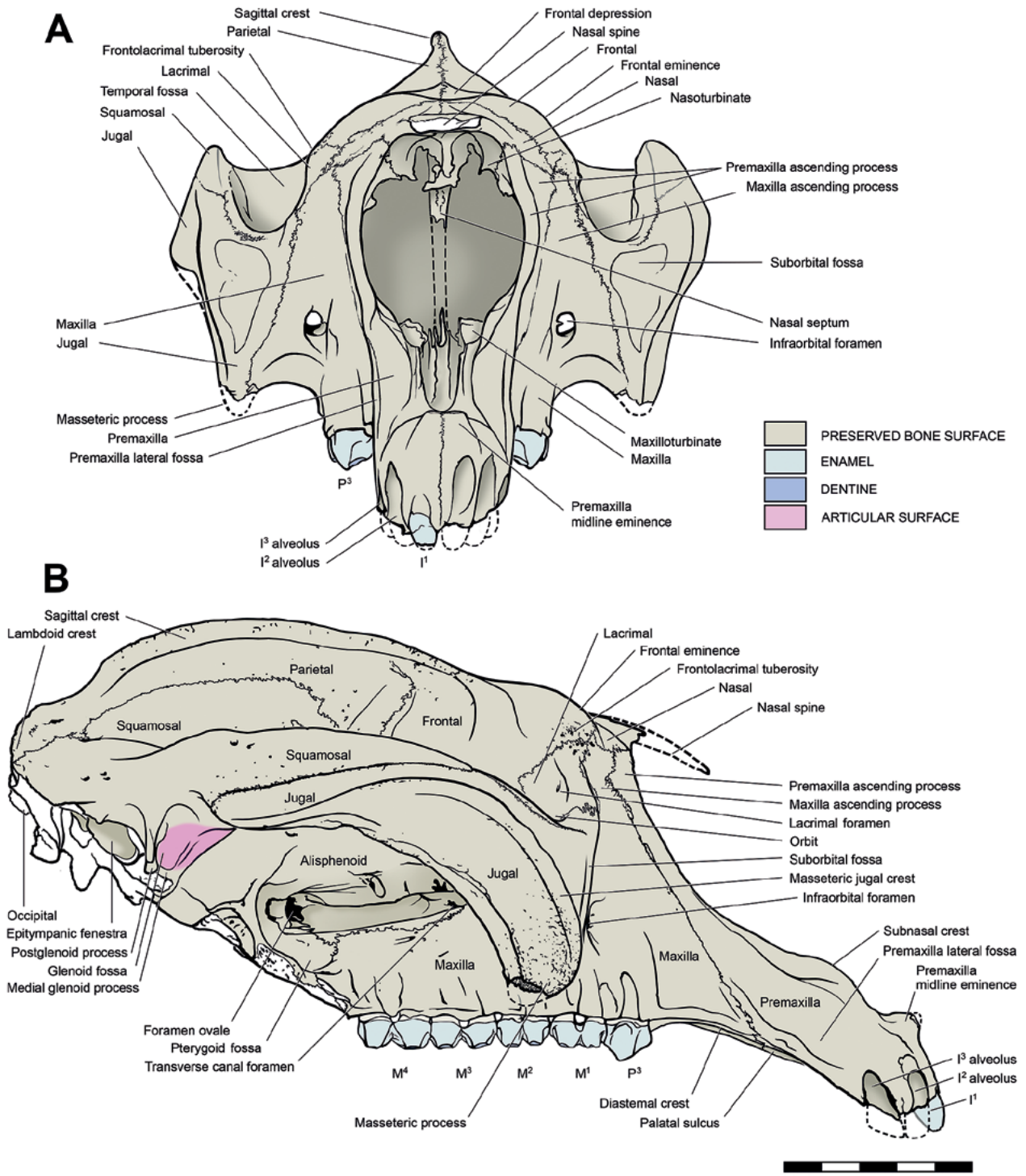

Figure 5. *Propalorchetes novaculacephalus*, measured cranium outline diagram based on QVM2000GFV459: a, anterior: b, lateral views of cranium; scale bar represents 5 cm.

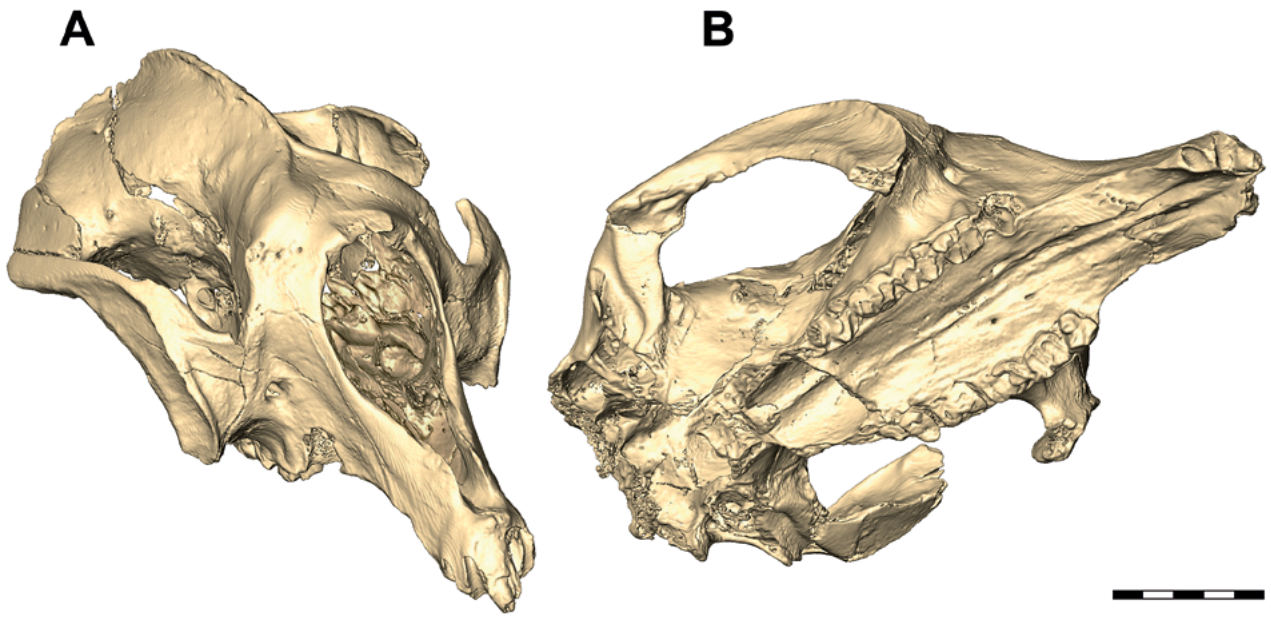

Figure 6. *Propalorchetes novaculacephalus* surface rendering based on CT scan data from QVM200GFV459; a. oblique anterodorsal view; b. oblique anteroventral view; labels indicate regions described; for interactive views, refer to the 3-D pdf in supplementary information; scale bar represents 5 cm.

level of the M^1 crown base. The tapering form suggests that the masseteric process of this specimen may not have projected below the base of the molar crowns, (figs. 5A–B).

Infraorbital foramina appear proportionally small compared to *Palorchestes* and smaller than those described by Murray (1990) for the *Propalorchestes novaculacephalus* paratype, NTM P862-27 (tables 1, 2). Slightly higher than wide (average maximum diameter 5.97 mm; average minimum diameter 5.47 mm), the rounded rectangular infraorbital foramen possesses a thin, horizontal baffle that projects from its medial wall. A facial fossa extending anteriorly along the lateral maxilla surface from the infraorbital foramen is only weakly evident in this specimen. Anteroventral to this is a long, shallow premaxilla lateral fossa. The ventral limit of this lateral fossa accentuates the line of the diastemal crest.

The premaxillary ascending processes that cap the long lateral nasal walls are expanded proximally with a convoluted suture to the nasals and maxilla as described above. A second 'flat' surface originates on the medial side of the distal half of the nasal wall. It becomes rounded as it rolls onto the lateral surface, but not as sharply as the narial notch above it. Proximally, this forms a sharp dorsal rim along the premaxilla ascending process at the widest part of the nasal aperture. Distally, this anteriorly directed surface forms a broader, rounded dorsal edge on the premaxilla as it becomes confluent with the lateral wall of the nasal aperture. In so doing, it effectively restricts the width of the nasal aperture. Between this second feature and the projecting root of the maxilloturbinate on the medial surface of the nasal wall, a third flat surface arises to run anteriorly. This surface becomes a shallow groove that also rotates onto the dorsal edge of the premaxilla to become confluent with the lateral nasal wall. The medial edge of this groove is raised into a sharp, thin, subnasal crest that forms a convex profile (approx. 24.7 mm long) to the proximal nasal rim when seen in lateral view. In dorsal view the subnasal crests are parasagittal and delimit the narrow anterior part of the nasal aperture (width 11.5 mm). At the anterior termination of each crest, the profile curves further ventrally to form a more rounded, but concave rim; defining the distal extent of the nasal cavity and rising to form the premaxilla midline eminence. The anterior of the nasal aperture is semicircular in dorsal view. The midline eminence is abraded, but enough remains to indicate it formed a higher, paired transverse peak across the midline. The posterior wall of the eminence bears two small pits. The premaxilla-maxilla suture forms a straight, oblique passage as it traverses anteroventrally from the dorsolateral edge of the nasal along the lateral rostral wall to the diastemal crest. On the ventral surface of the diastema, the premaxilla-maxilla suture turns sharply posteromedially before abruptly running anteromedially to the incisive foramen within the palatal sulcus. On the lateral wall of the sulcus the premaxilla projects posteriorly to form each incisive foramen and the incisive process that separates them. The incisive process also forms a rounded midline ridge that deeply divides the palatal sulci along the ventral premaxilla. Ventrally, the maxilla contributes only to the posterior end of the incisive foramen. Dorsally, the morphology is the converse; the maxilla forms an incisive process that projects anteriorly to form the medial walls of the incisive foramena and expands slightly over the midline within the nasal cavity for a further 6.4 mm. Posteriorly from this point, the maxilla forms the sharply raised sulcus that would have accommodated the

vomeronasal (Jacobson's) organ, the ventral insertion for the nasal septum and the vomer (see below). The palate is flat, except for the palatal sulcus that shallows and narrows from a point opposite the anterior moiety of M^1. The midline suture forms a slight ridge in this region. Two anterior palatal foramina are positioned slightly asymmetrically lateral to the edge of the palatal sulcus, adjacent to the M^1. Minor foramina are similarly laterally sited posterior and anterior to these. The maxilla-palatine suture is highly convoluted, commences at the midline opposite the interloph valley of M^3 and arcs anteriorly before running posteriorly beside the posterior moiety of M^3 and the M^4. On the right, the suture meanders increase in lateral-medial amplitude before descending into the posterior palatine foramen. The foramen lies immediately posterior to, and aligned with, the medial edge of M^4 and opens into a slightly anteromedially directed trough that extends to a position level with the M^4 metaloph. The remaining posterior surface morphology and posterior palatine rim is not preserved.

The premaxilla rostral tip contained three pairs of incisors in a semicircular arc with the incisive portion of the palatal sulci extending anteriorly to the I^1 alveoli. The I^3 alveolus is the largest, av. 12.07 mm diameter, and forms a lateral sub-terminal swelling that widens the rostrum. Some surface is lost at the premaxilla tip and about the alveoli, but the curved, anterior face preserves a shallow concave fossa above the right incisor alveoli. This would also have been a paired feature of the rostral tip. The root and crown base of the right I^1 remains; the left I^1 alveolus is 5.76 mm in diameter. The I^2 alveolus is intermediate, av. 6.58 mm diameter.

Cranial roof. In lateral view, the dorsal profile of the neurocranium is high and strongly convex due to a prominent sagittal crest (maximum height approximately 5.5 mm, horizontal length approximately 100 mm, circumference length, approximately 120 mm). The crest is formed entirely by parietal; there is no indication of an interparietal, but the posterodorsal region of the skull is well fused. Woodburne (1967b) was unable to define the cranial sutures in the occipital region for *P. painei*. The crest reduces sharpness posteriorly as it divides at the occipital to form the laterally curving, lamboidal crests.

Cranial walls. There are several irregularly positioned foramina on the dorsolateral parietal and squamosal surfaces that follow the line of the lamboidal crests. Murray (1986, figs. 2–4A, C) identified similar foramina on the left of holotype NTMP8552-10, but they are highly asymmetric on QMV2000GFV459. The parietal and squamosal contribute equally to the swollen ovoid form of the posterior part of the neurocranium. Murray (1986, pp. 202–3) remarked that the general morphology of the neurocranium of *Pr. novaculacephalus* was didelpid-like with respect to its crested, narrowly waisted and ovoid character, but added this was likely a derived state in *Propalorchestes* and not a plesiomorphic condition.

The glenoid region is well characterized by Murray's description of the holotype (Murray, 1986, p. 199). It is consistent with the morphology of QVM2000GFV459, particularly the more complete, right side of the specimen. The roughened surface irregularities of the jugal and its lateral glenoid process confine the anterolateral extent of the articular surface. The glenoid fossa is essentially a transverse groove along the posterior boundary of the shallowly concave anterior articular surface. It is bounded mesially by the oblique ventral projection of the medial glenoid process and opens laterally between the transversely oriented postglenoid process and the lower ventral plane of the anterior articular surface. A pair of fine creases on the anterior articular surface of the squamosal, delimit the transverse boundary between the two. These creases are very slightly curved anterolaterally towards the jugal, as Murray (1986) detailed, and form a very shallow groove between them (fig. 3B). The lateral half of the postglenoid process preserves a more ventral and distinctly anteriorly rolled crest. The rim of the crest is rugose and further confines the articular region. Murray (1986) did not mention this distinctive morphology, presumably because, if present, it was lost through damage.

Only small anterior portions of the pterygoids remain of the basicranial region and are sheathed anteriorly by the extensive vomerine surface within the choanal orifice. The median septal plate of the vomer is partly preserved. The squamosal-alisphenoid suture cannot be followed posteriorly from the medial glenoid process due to breakage and loss.

The zygomatic arch projects directly anteriorly from the posterior zygomatic root in both the holotype and QVM2000GFV459 whereas it arcs anterodorsally in *P. painei* and the curvature continues to the ventrally extended tip of the masseteric process. The excavation of the lateral jugal surface of the zygomatic arch is pronounced and covers a greater proportion of its surface than in *P. painei*. The anterior extremity of the squamosal on the dorsal edge of the zygoma has been damaged. The frontal process of the zygoma cannot be seen in this thin region and was probably relatively slight. The damage and some over-etching of the squamosal-jugal suture has resulted a highly convoluted extension of the suture that continues along each orbital rim, almost to the lacrimal suture. The medial surface of the arch bears four shallow depressions.

Cranial rear. The proportion of the occipital region preserved in QVM2000GFV459 is similar in area to that of the *Pr. novaculacephalus* holotype, but represents the dorsal half only, compared to the near complete left half in the holotype. Furthermore, the new specimen has lost most of the remaining external occipital surface. This prevents reconstruction of the occipital region in QVM2000GFV459 and restricts comparison with the taxonomically significant basicranial and condylar anatomy of the holotype. The general proportions and plane of the occipital plates in both specimens compare favourably (occipital plane of QVM2000GFV459 96.5° posterior to occlusal plane; NTMP8552-10 estimated to be 100.0°) and the right suboccipital fossa was strongly concave and well separated by a midline ridge (figs. 7, 9).

Endocranial Sinuses. Using the CT data, some auditory and most non-auditory sinuses can be examined and compared with the original holotype description and illustration of Murray (1986, fig. 4). A graphic overlay is provided (fig. 7C).

The paired epitympanic sinuses that lay immediately dorsolateral of the cerebellar region of the endocranium are exposed by posterior breakages (figs. 3B, 7B, C, 8A, B, C, E).

They appear to not extend as posteriorly as those in the holotype partly for this reason. The posterior parietal sinus location indicated by Murray (1986, fig. 4b, d) is also more posterior to that of QVM2000GFV459. Several irregular vacuities can be seen in this location (mostly right of the midline), but some represent damage and losses. The graphic comparison presented in figure 7C indicates that there is a slight discrepancy in the angle of view between that of Murray (1986) and our own, which has resulted in the relative posterior displacement of all sinus features of the holotype in respect to those of QVM2000GFV459. The parietal sinus was an extensive volume that occupied all of the dorsal and dorsolateral expansion about the endocranium. In dorsal outline it was slightly asymmetric and paired. The broad lateral sinus expansions only relate in part to those figured by Murray (1986, fig. 4D) (fig. 7C). The sinus schema he elucidated for the endocranial cavities aligns with the new material, but the scan provides insights permitting an alternative interpretation of the anatomy. The large sinus that shrouds the endocranial cavity of the brain beneath the parietals, is the parietal sinus and not the frontal sinus as originally designated by Murray (1986), but accords with anterior and posterior views of the natural breakage of the holotype in Murray (1992, figs. 2A, B). The sinus volume includes a large posterior lobe along the midline and posterolateral flanges that correlate to the "posterior-" and "anterior parietal sinuses" respectively of Murray's (1986) holotype description. These do not appear to be independent in QVM2000GFV459. The lateral expansion within the parietal extends beneath the parietal-squamosal suture line on the lateral surface of the skull and the sinus floor closely abuts the anterior epitympanic sinus (figs. 7C, 8, 9).

A paired anteroventral chamber of the parietal sinus closely abuts the posterior portion of the frontal sinus. It is united via a sagittal passage from the mid point of the main parietal chamber floor to its ventral half. The floor of this passage forms the very thin roof of the cerebral portion of the endocranial chamber. The anteroventral parietal sinus lies dorsal to the olfactory bulbs and is aligned with the serial divisions of the frontal sinus above the cribiform plate (fig. 9A, supplementary 3D interactive pdf).

Only the dorsal parts of the auditory sinuses remain in QVM2000GFV459. Dorsal to these, a small horizontal supraoccipital sinus surmounts each epitympanic sinus and runs anterolaterally to contact the posterolateral end of the parietal sinus with its anteromedial corner. The supraoccipital sinus identified in the holotype is depicted entirely medial to the epitympanic sinus, but in the new specimen, a, large posterior epitympanic sinus projects posteriorly from beneath it. A vertical strut incompletely partitions the posterior portion of the epitympanic from a more voluminous anterior epitympanic sinus. These are partially exposed by the loss of the basicranium. The most anterolateral extensions of the sinuses, including the glenoid hypotympanic sinus, are preserved within the posterior root of the zygoma.

The frontal sinus is chambered. Its asymmetry is pronounced, but does not obscure the basic pattern of paired transverse divisions of the volume that extends from a point level with the frontal-parietal suture at the cranial "waist" to the midline point of the frontal-nasal suture. The most posterior chamber lies ventral to the main parietal sinus, separated from it by irregularly thick, bony walls. A large lateral frontal sinus diverges anterolaterally from beside the second anterior frontal chamber to occupy the volume beneath the frontal crests and frontal eminence. Thus, the lateral frontal sinus extends well forward of the midline chamber series to terminate posterior to the frontolacrimal tuberosity.

In addition to the frontoparietal sinuses, maxillary sinuses are also evident (figs. 8D, E). They are highly asymmetric; the right side is three times the volume of the left and extends to the maxilla-jugal suture. Their volume is subdivided (or isolated) and appears to represent a lateral elaboration of the maxillary sinus. Structurally, this relates to the vertical expansion of the anterior root of the zygoma and facial surface. This is similar to the lateral squamosal sinus elaboration above the glenoid with the widening (horizontal expansion) of the posterior zygoma (see p. 14). The degree of sinus development shown in *Propalorchestes* is strong and significant in relation to the allometric trends and specializations of later and larger Vombatomorphia (Murray, 1992; Sharp, 2016). An indication of the evolutionary development of the sinus system and corresponding increase in skull size can be gained by the comparative outline featuring *P. azael* (fig. 9). The volume of the endocranial cavity has remained reasonably constant despite the five fold increase in skull volume, indicating the extreme degree of negative allometry of the brain.

Nasal cavity – The voluminous cavity is divided by a stout ethmoidal nasal septum. A thick and osseous dorsal pedestal attaches to the ventral surface of the nasals. Bony lateral expansions are preserved on the medial lateral walls of the maxilla, midway between the premaxilla midline eminence and the base of the nasal spine. These served as the attachment sites for the extensive maxilloturbinates (Fig. 9A). The ventral edge of the septum was located in an elevated median trough on the cavity floor and the anteroventral extent of the septum, whether ossified or cartilaginous, was confined by the base of the premaxillary midline eminence. Fragments of the ethmoturbinates remain against the cribiform plate. The location of the nasoturbinate scroll can be seen bridging the nasal and dorsomedial surface of the proximally flared premaxilla process. The dorsal outline of the cavity is proportionally wider than *P. painei* both with respect to the parallel-sided anterior part and the expanded, heart-shaped proximal portion of the cavity. The cavity is slot-like in *P. painei* where the proximal portion is more triangular, the central region slightly laterally curved and the distal third parallel-sided. The nasal cavity length proportions for both *Pr. novaculacephalus* and *P. painei* represent one third of their skull length. *Propalorchestes novaculacephalus* has a gently concave profile to the lateral wall of the nasal cavity because the subnasal crest and the narial notch (lateral to the nasal spine) is less incised. In dorsal aspect, *Pr. novaculacephalus* is morphologically similar to *P. azael,* but proportionally, the nasal cavity is half the skull length in *P. azael*. In anterior view *Pr. novaculacephalus* has proportionally the widest oval-shaped aperture, *P. azael* is intermediate in being narrowly triangular and *P. painei* the narrowest and more parallel-sided.

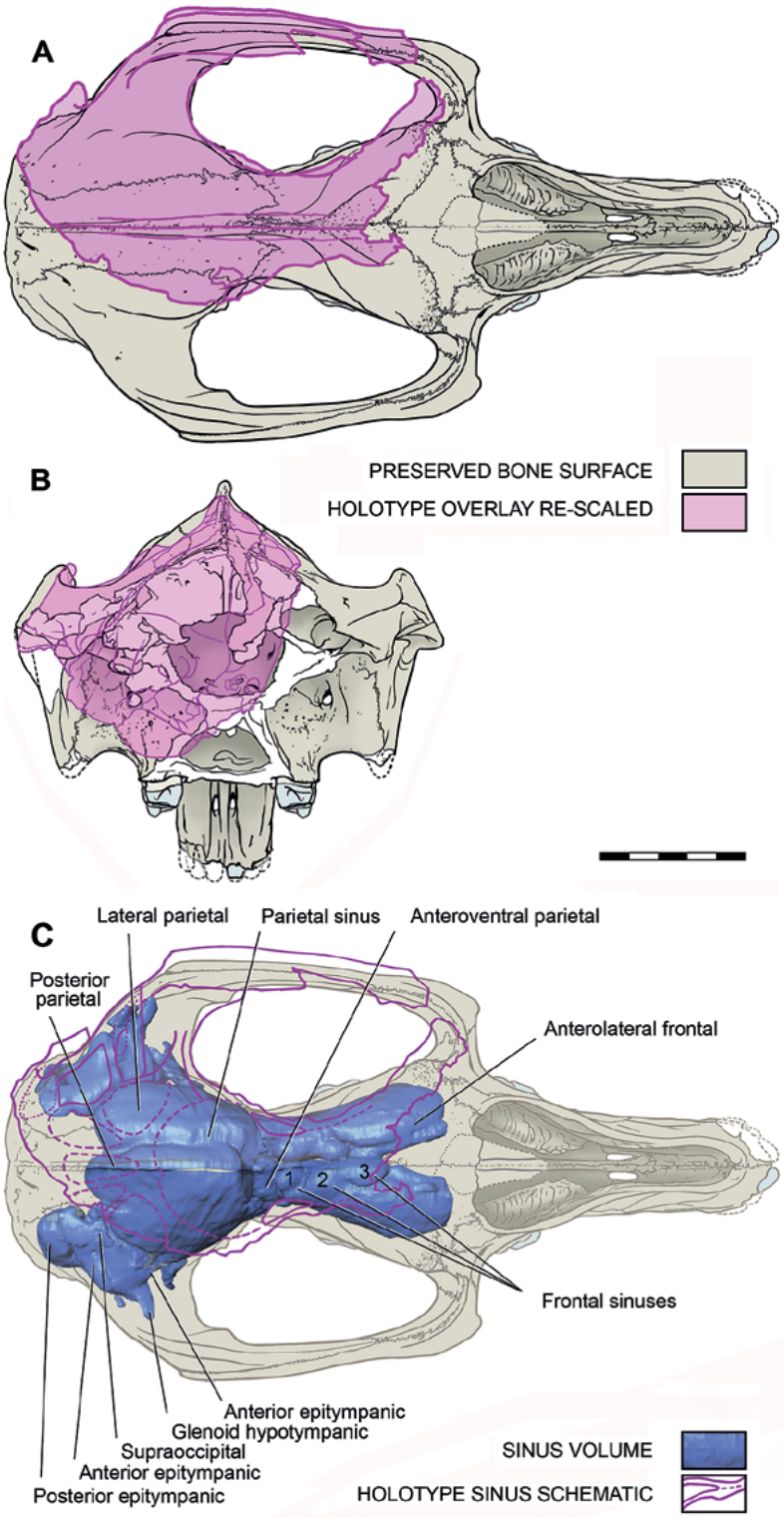

Figure 7. *Propalorchestes novaculacephalus* QVM2000GFV459 reconstructed outline with translucent overly of *Pr. novaculacephalus* NTMP8552-10 holotype cranial fragment, not to scale - holotype reduced by 90% to compare form, based on data from Murray (1986, Figs. 1, 2b, 3); a, dorsal view; b, posterior view; c, dorsal view including sinus volume rendering from CT data and schematic diagram overlay of holotype sinuses based on Murray (1986, Fig. 4d), note - outline graphic of NTMP8552-10 shows some posterior displacement; scale bar represents 5 cm for QVM2000GFV459 only.

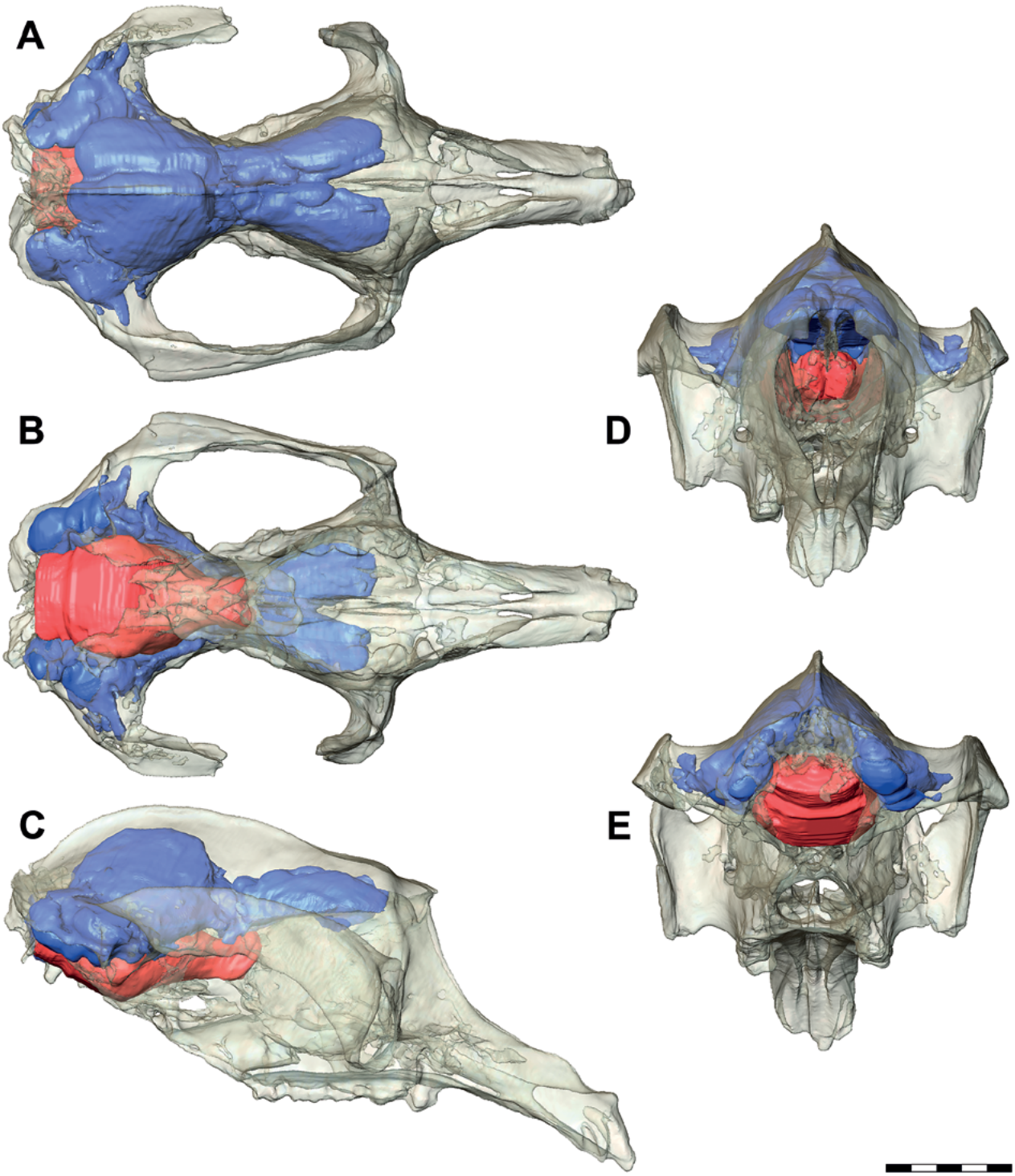

Figure 8. *Propalorchetes novaculacephalus* endocranial and sinus volumes rendered by digital segmmentation of CT scan data from QVM200GFV459: a. dorsal; b. ventral; c. lateral; d. anterior; e. posterior views; endocranial cavity red; auditory, squamosal, parietal and frontal sinuses blue; labels indicate regions described; scale bar represents 5 cm.

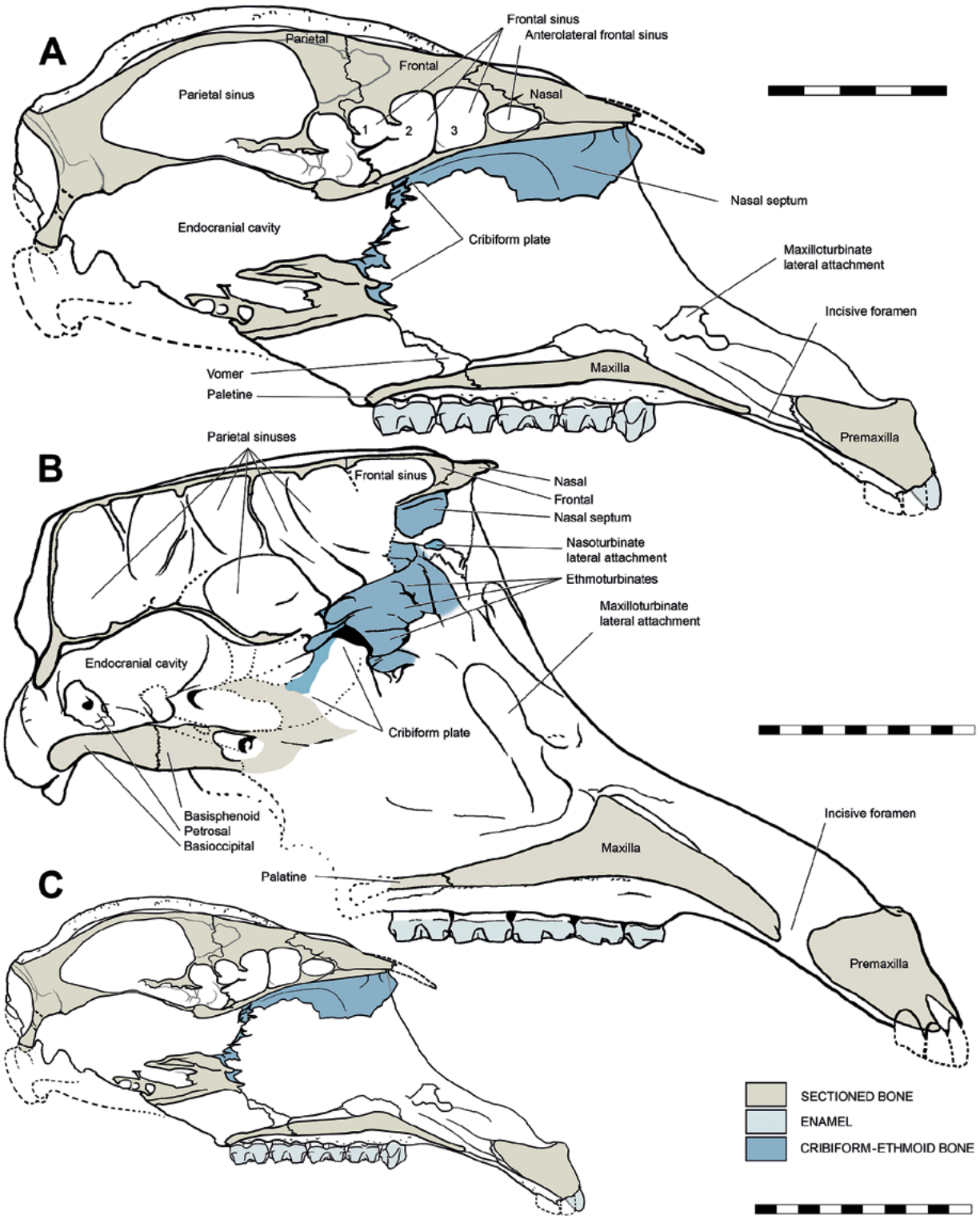

Figure 9. *Propalorchetes novaculacephalus* reconstructed cranial sinus outline compared with *Palorchestes azael* as revealed in parasagittal section taken immediately left of midline to exclude sagittal septa: a, *Propalorchetes novaculacephalus* QVM2000GFV459 based of CT scan data; scale bar represents 5 cm: b, *Palorchestes azael* NMVP216490 represented at the size of *Pr. novaculacephalus* 9a, based on exposures of cranial fragments and CT scan data; scale bar represents 10 cm: c, *Propalorchetes novaculacephalus* QVM2000GFV459 represented to scale of *P. azael* NMVP216490 in 9b; scale bar represents 10 cm.

Dentition. Cusp nomenclature for *Propalorchestes* follows Rich and Archer (1979) and Murray (1990) wherein: the protoloph is composed of buccal stylar cusp C and the lingual protocone; and the metaloph is composed of a buccal stylar cusp D and a lingual metaconule. Both the paracone and metacone are subsumed into the protoloph and metaloph respectively (Black, 2006). Note that the hypocone described by Woods (1958) and Woodburne (1967) for *Palorchestes* is probably homologous to the metaconule (Murray and Wells, pers. comm.) (See fig. 13 for *Propalorchestes* upper dentition showing terminology).

A composite description for the *Propalorchestes* dentition will be provided drawing upon the QMV2000GFV459 skull and QMV2000GFV406 mandible (figs. 12, 13A–B & 16).

dP^3: not expected for the age of the QMV2000GFV459 specimen and an isolated dP^3 has yet to come from the Bullock Creek LF. Refer to Black (2006) for a detailed description of the dP3 from a juvenile maxilla, *Pr. novaculacephalus* QMF50605, Jim's Carousel LF, Riversleigh WHA.

P^3: sub-triangular in occlusal view; bicuspid crowned; tri-rooted; and wider than long. The crown bears a large central parametacone and a large lingual protocone. The moderately worn QMV2000GFV459 left P^3 occlusal morphology (fig. 13A) compares favourably with the unworn *Pr. novaculacephalus* P^3 QMF50605 from Riversleigh.

Three crests extend from the parametacone of QMV2000GFC459: 1) a short anterobuccal crest, which fades down the steeply sloping buccal face and provides a lateral lobe on the parametacone occlusal wear facet outline; 2) A short anterolingual crest produces an anterolingual lobe of wear; and 3) A prominent posterobuccal crest, descends steeply to the base of the crown, produces a large posterior lobe to the wear outline. The occlusal wear from the posterobuccal and anterolingual crests is aligned with the steep-sided valley separating the parametacone and protocone.

The protocone apex shows a small wear facet that incorporates two crests in outline: 1) a weak anterobuccal crest opposes the anterolingual crest of the parametacone in the interloph valley; 2) a posterobuccal crest runs parallel to the posterobuccal crest on the parametacone. A posterolingual cingulum extends from the base of the posterobuccal parametacone crest to the lingual base of the protocone, forming a posterolingual cleft from which the posterobuccal protocone crest decends. A weak posterobuccal ridge extends from the base of the posterobuccal parametacone crest, confluent with a posterobuccal cingulum that curves anteriorly around the tooth margin and fades into the base of the crown opposite the parametacone apex. This cingulum forms a broad cleft on the posterobuccal face of the parametacone that separates its two buccally directed crests. Black (2006) described a sub-apical crest on the anterobuccal face of the parametacone that curves lingually around the base of the tooth. This is strongly indicated on QVM2000GFV459 by a sharp extension of the parametacone wear facet that extends to the base of the anterobuccal corner of the parametacone. From this point a short ridge extends posterobuccally, while a faint precingulum wraps posterolingually on the anterior tooth base. The pre- and postcingulum morphology is more extensive than QMF50605, but this may be indicative of the under developed, un-erupted condition of the QMF50605 P^3. The crown of P^3 extends well below the occlusal line of the upper molars and it's degree of wear is significantly less than M^1; (the occlusal area of the P^3 wear facets are closer to the wear extent on the M^4 metaloph).

Upper molars are roundly sub-rectangular to trapezoidal in occlusal outline and bilphodont, consisting of a protoloph (connecting the protocone, paracone and stylar cusp C) and a metaloph (connecting the metaconule, metacone and stylar cusp D). (figs. 13B, 16). The protoloph and metaloph are slightly crescentic, recurved posteriorly, but to differing extents. Stylar cusp C is posterior to the paracone and stylar cusp D is sharply deflected posteriorly. There is posteromedial buttressing of the protocone and metaconule. The interloph valley is deep, V-shaped in profile and partially bridged by a "proto-midlink," corresponding to the midlink that connects paracone to metacone in *Palorchestes* (Mackness, 1995). Precingulum, postcingulum and lingual cingulum are present, but there is no buccal cingulum. A weak to moderate forelink (or preparacrista) extends from a weak stylar cusp B towards the paracone and a postlink (or postmetacrista) extends from a stylar cusp E towards a point between the metacone and metaconule. All "links" are positioned buccal of the crown midline to varying extents. Both the fore- and postlinks confer slightly extended, less rounded corners to the buccal face of the crown in occlusal view; these correspond with stylar cups B and E, respectively. The presence of a lingual cingulum gives a straighter, less "waisted," outline to the lingual face in occlusal view and squarely confines the interloph valley in medial view. By comparison to the crown ornament of *Palorchestes* species, wrinkled to pustular ornament is only weakly present in the clefts of the cingula and interloph valley in *Propalorchestes* (fig 12).

The morphological progression of the upper molars is as follows: 1. The size gradient for length and width is sub-equal from M^1-M^3, but the M^4 of QVM2000GFV459 is longer and narrower. 2. The length of the protoloph compared to metaloph near the crown base increases from sub-equal for M^1 to approximately 125% of the metaloph on M^4. 3. The width of protoloph usually greater than metaloph. 4. The extent of occlusal wear is always greatest on the "thicker" protoloph. 5. The anterior face of both lophs is more steeply inclined than the corresponding posterior face. 6. The length of the interloph valley increases slightly from M^1-M^4. 7. The prominence of all "links" (or cristae) generally decreases from M^1-M^4. 8. Crown outline in occlusal view for M^1 is trapezoidal with buccal side longest, M^2 more rectangular, M$^{3-4}$ increasingly trapezoidal with the lingual side increasingly the longest (fig. 16).

The degree of wear on QVM2000GFV459 **M^1** precludes an indication of original relative cusp heights. The morphology compares most closely with the *Pr. novaculacephalus* paratype NMTP862-27 (Murray 1990, fig. 3); (figs. 12B, 13). In regard to the individual cristae on the crown, the "forelink" or preparacrista is prominent and extends to the anterolingual margin of the crown as in QMF50605. The "postlink" or postmetacrista also compares well with QMF50605, QMF51399 and QMF30844, but is more extensive and further buccally directed than in these Riversleigh specimens. In the

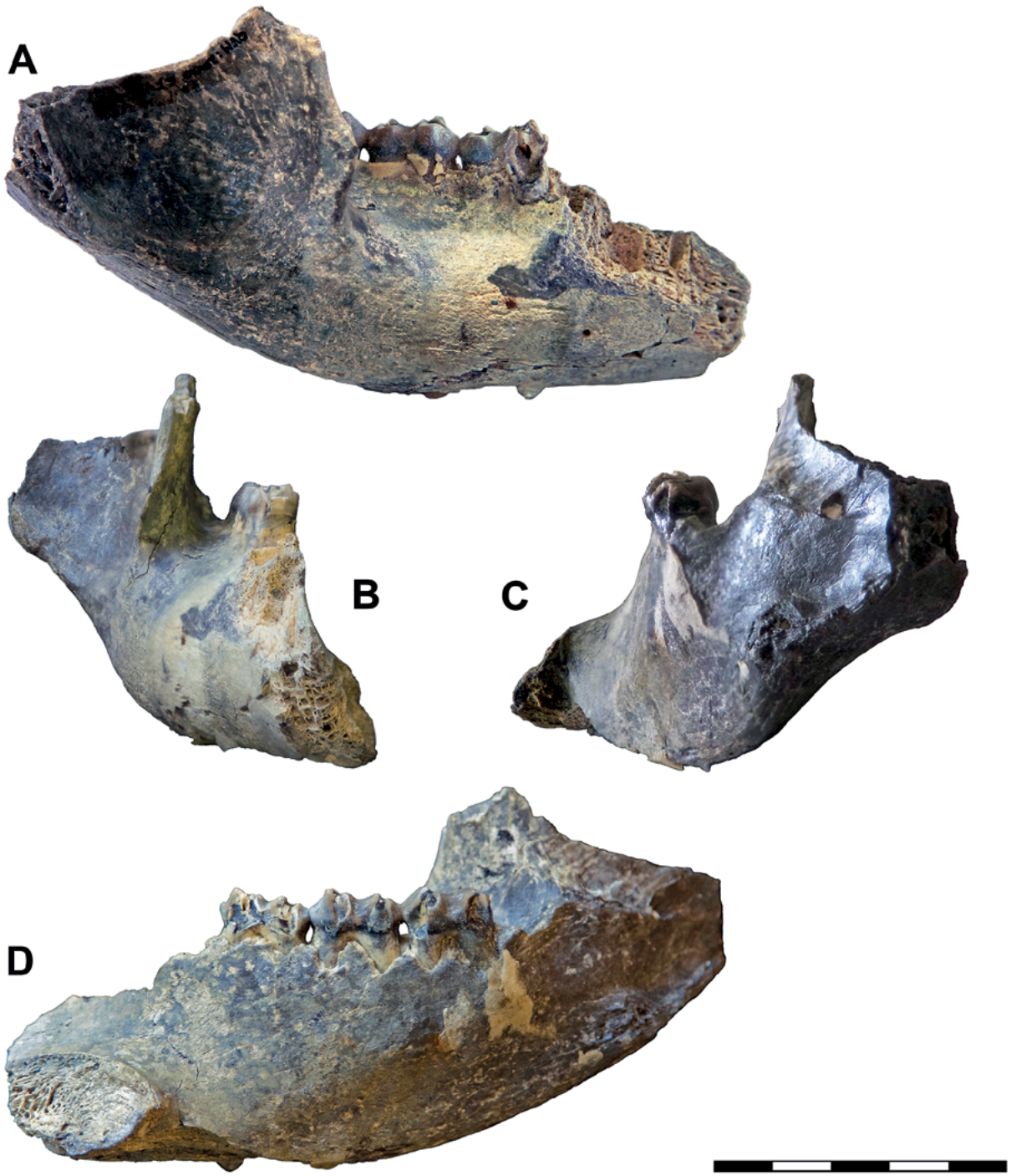

Figure 10. *Propalorchetes* cf *novaculacephalus* QVM2000GFV406 right mandiblular fragment: a, lateral: b. anterior: c, posterior: d, medial views, (not corrected for parallax); scale bar represents 5 cm.

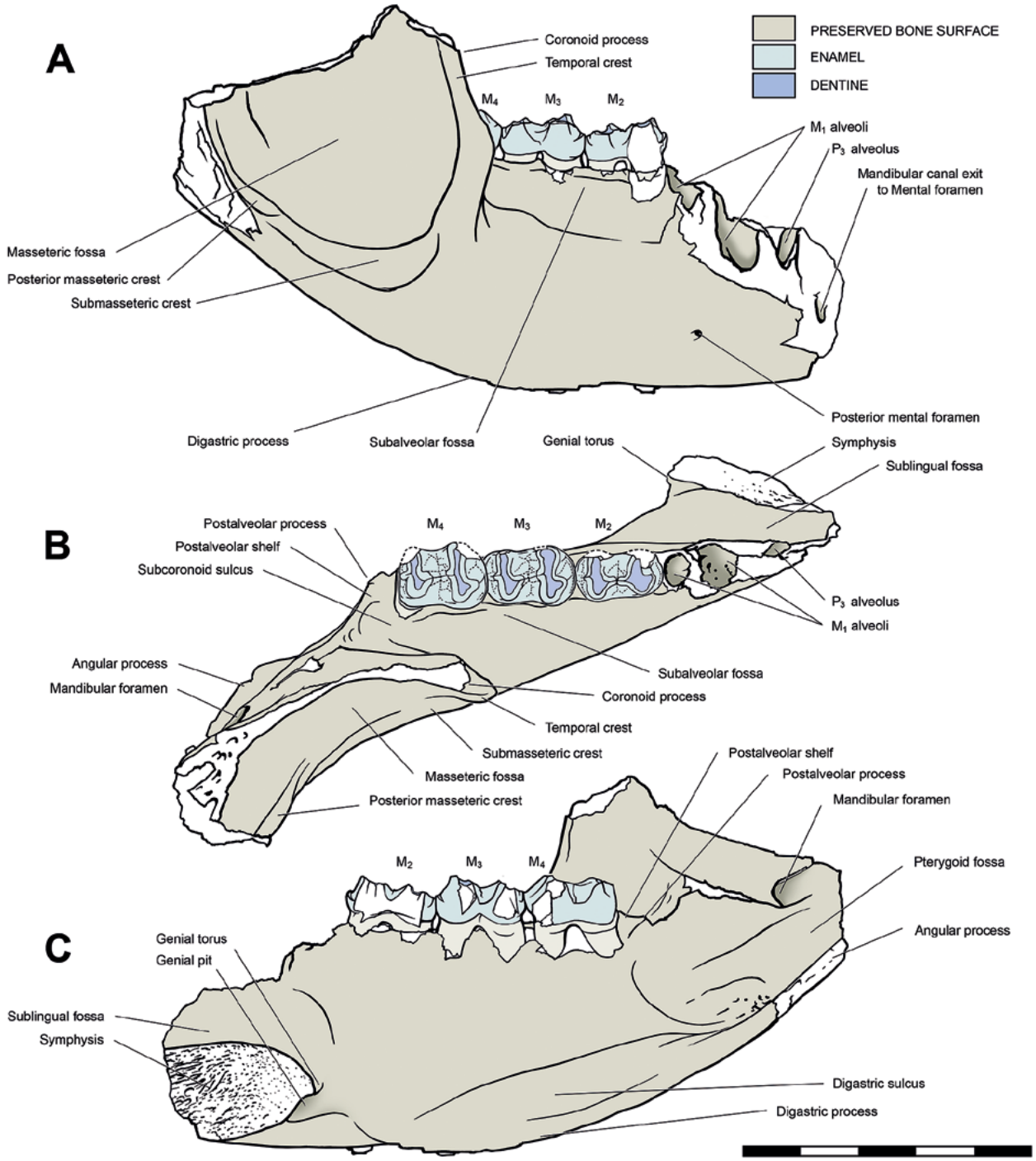

Figure 11. *Propalorchetes* cf *novaculacephalus* QVM2000GFV406 measured mandibular outline diagram: a, lateral: b, medial: c, occlusal views; scale bar represents 5 cm.

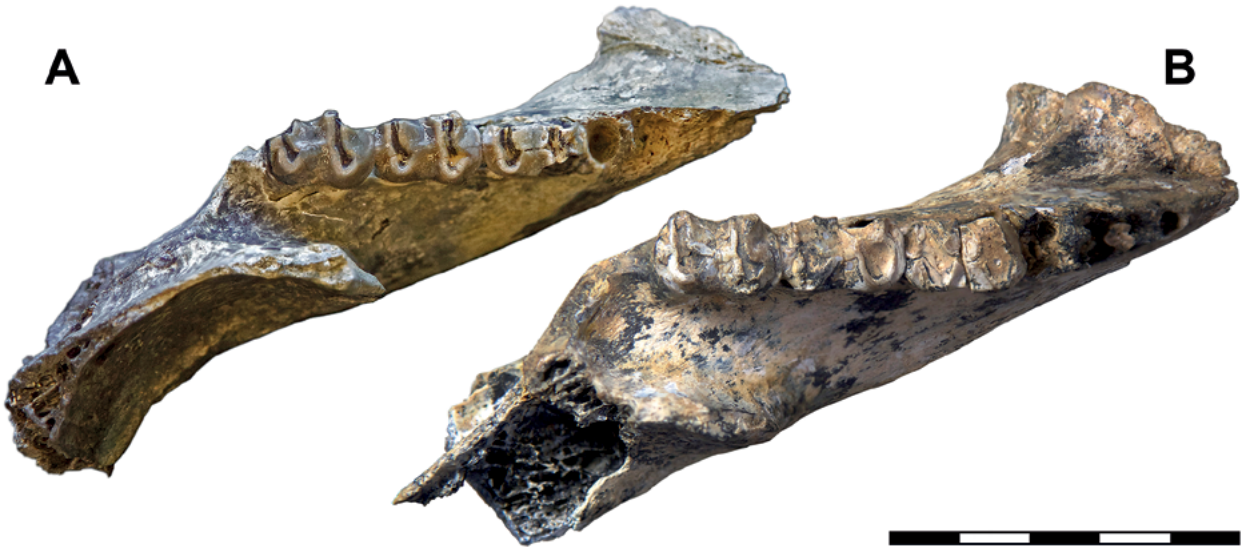

Figure 12. *Propalorchetes* mandiblular specimen comparison in occlusal view: a, *Propalorchetes cf novaculacephalus* QVM2000GFV406 right mandiblular fragment; b, *Propalorchetes novaculacephalus* NMVP187282 paratype right mandiblular fragment (not corrected for parallax); scale bar represents 5 cm.

QMF51399 and QMF30844, the "postmetacrista" is incipient and not confluent with stylar cusp E. In all specimens, a postparacrista extends posteriorly into the interloph valley where it meets a weak, short, anterior crest at the base of the metaloph at a point opposite the metacone apex. This "proto-midlink" is prominent in the new material and the paratype NTMP862-27, but less developed in the Riversleigh specimens. On QVM2000GFV459, the loph wear facets almost unite across this structure on the right M^1, whereas it does bridge the loph wear on the left M^1. There is a second incipient bulge, medial to the metacone, on the anterior metaloph face, that is also present on NTM682-27, but is either less developed or not evident in the Riversleigh material (fig. 13, refer also to the M^2 description below). Pre-, post- and lingual cingula are strongly developed and of sub-equal size for all specimens.

M^2 is similar to M^1, but has a narrower and less steeply sided metaloph that ultimately wears to produce a parasagittaly wider wear facet than M^1. The interloph valley is also less steeply sided and forms a broader cleft with the lingual cingulum. The right QVM2000GFV459 M^2 has an equally pronounced, second anterior bulge, medial to the first, at the base of the metaloph and a slightly weaker one opposing it on the posterior surface of the protoloph. This closely matches the morphology in the paratype NTM682-27 M^1 for which Murray (1990, p. 41) described the structure as a centrocrista and a pair of bulges separated by a rhomboidal fossa in the interloph valley. QMF50605 M^1 and M^2 also have a less pronounced version of this morphology and together both features are probably the precondition for the double midlink developed in later *Palorchestes*. The combination of this structure and the less inclined interloph valley ultimately produces M^2 loph wear facets with a double connection and a circular to rhomboidal fossa between them (fig. 13). This is commonly seen in the wear conditions in *Palorchestes* dentition. The second *Pr. novaculacephalus* paratype, QMF12429 compares least favourably with QVM2000GFV459, QMF50605 or NTM682-27, because there is no indication of the second bulge on the anterior face of the metaloph and the postparacrista is weak and not well aligned with the single crest at the anterior base of the metacone (fig. 13). This constitutes the weakest indication of a "proto-midlink" of all the *Propalorchestes* material. If it is regarded as an M^3, the identity of QMF12429 remains questionable.

The preserved right **M^3** continues to show a small proportional reduction in the metaloph by comparison to the protoloph and a slightly reduced steepness to the posterior faces of both lophs. The postmetacrista is reduced in size, descends only half way to the metacone and is less markedly directed towards the posterobuccal corner of the crown. Although the specimen is broken in this region and the remaining morphology has a more prominent relief, it compares favourably with the proportional changes seen in the QMF50605 tooth row and indicates that the postmetacrista, stylar cusp E and the "proto-doublelink" morphology are all positioned less buccally than M^2 and M^1. The postcingulum is reduced in proportion to the reduction of the M^3 posterior moiety. Due to breakage, the lingual cingulum is missing. The precingulum, stylar cusp B and "forelink" remain well developed and the latter cusp and crista retain the anterobuccal position.

M^4 continues the proportional reductions in crown morphology, but the remaining right tooth on QMV2000GFV459 has lost the buccal 1/3 of the protoloph and the posterior surface of the metaloph has been sheared off. The postparacrista is a distinct, high crest; the interloph valley is wider, its cleft is more crenulate and it features incipient double bulges at the anterior base of the metaloph. The lingual

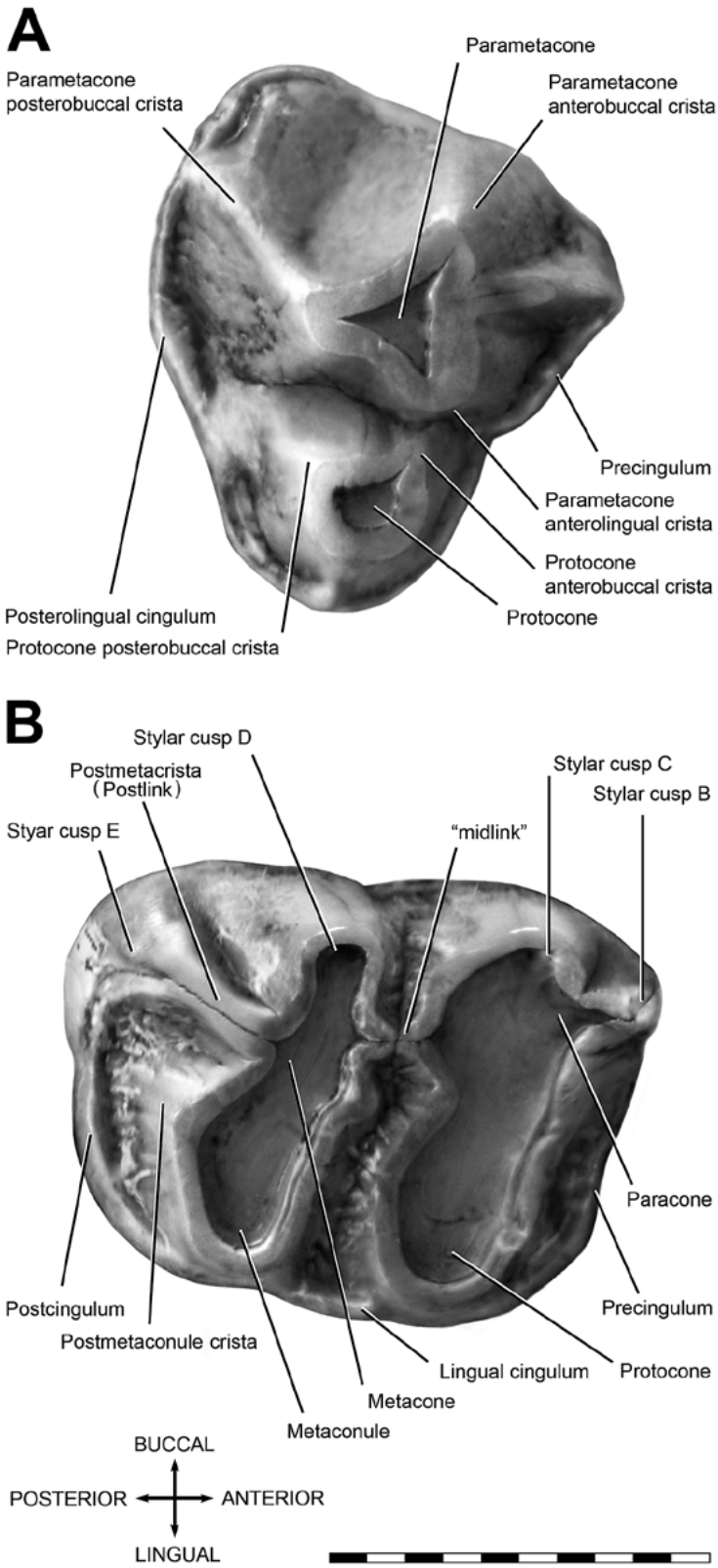

Figure 13. Digitally restored illustrations of the new Bullock Creek dental material with morphological features annotated: a, QMV2000GFV459 P^3; b, QMV2000GFV459 M^1; scale bar represents 10 mm.

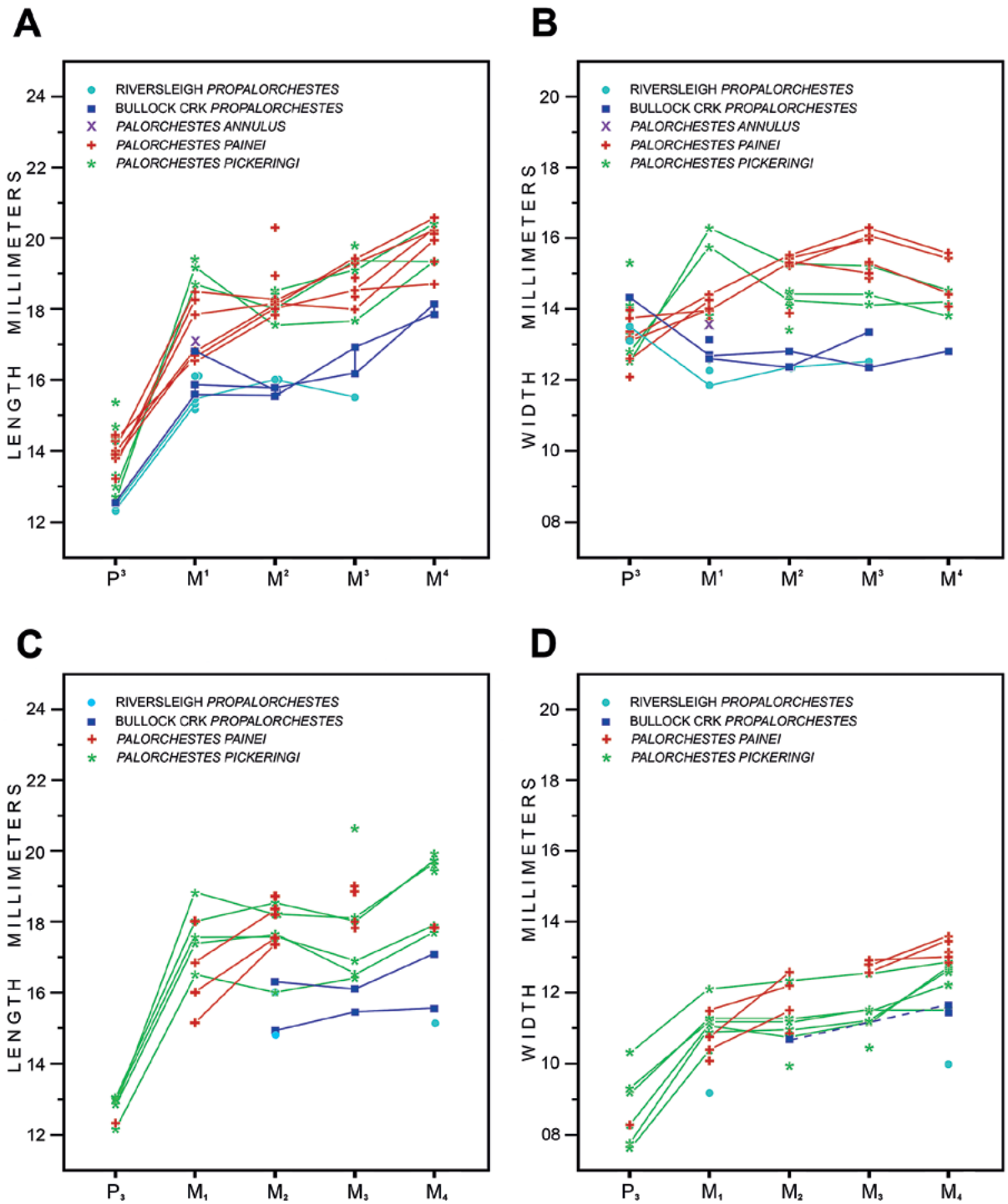

Figure 14. Dental measurements for *Propalorchestes* check teeth plotted with those of smaller *Palorchestes*: a, length upper cheek teeth; b, anteriorloph width upper cheek teeth; c. lower cheek teeth; d, anteriorloph width lower cheek teeth; data points that represent measures for successive teeth of the same tooth row are connected by a line; data points that represent measures for non-successive teeth of the same tooth row are connected by a dashed line; Data and sources provided in Table 2.

Table 3. Selected mandibular measurements for *Propalorchestes* (mm)

Specimen	**NMVP187282**	**QVM2000GFV406**	**QMF12430 (AR1779)**	**SMG1008**
Locality Site	Bullock Creek HW	Bullock Creek Top	Riversleigh D-site	Riversleigh Sticky-beak
Ramus depth @ M_2 protolophid	46.6	38.5	43.5	43.5
Ramus width @ M_2 protolophid	23.2	20.7	-	20.0
Symphysis width @ M_1 protolophid	29.8	24.3	25.5	28.0
Intercoronoid sulcus width	143.1	89.5	-	-
Data source	Trusler&Sharp	Trusler&Sharp	Murray 1990	Murray 1990

Table 4. Comparative mandibular measurements between *Propalorchestes* specimens expressed as percentages.

Specimen	**NMVP187282**	**QVM2000GFV406**	**QMF12430 (AR1779)**	**SMG1008**
Locality Site	Bullock Creek HW	Bullock Creek Top	Riversleigh D-site	Riversleigh Sticky-beak
depth cf NMV187282	-	83%	88%	88%
depth cf QVM2000GFV406	121%	-	107%	107%
depth cf SMG1008	107%	86%	100%	-
depth cf AR1779	107%	86%	-	100%
width cf NMV187282	-	89%	-	86%
width cf QVM2000GFV406	112%	-	-	97%
width cf SMG1008	116%	104%	-	-
Symphysis width cf NMV187282	-	81%	87%	94%
Symphysis width cf QVM2000GFV406	123%	-	105%	115%
Symphysis width cf SMG1008	106%	87%	89%	-
Symphysis width cf AR1779	117%	95%	-	110%
Intercoronoid Sulcus width cf. NMV187282	-	62.5%	-	-
Intercoronoid Sulcus width cf. QVM2000GFV406	160%	-	-	-

cingulum is longer with a wider, shallower, forked cleft. The buccal side of the interloph valley may also be slightly enclosed, but the fractured surface precludes determining the possible presence of a weak buccal cingulum.

Re-examination of the prepared material from Bullock Creek held by MV has revealed two further isolated dental fragments. The first specimen, NMV P249851 (No. 2329) from HW, appears to be a slightly worn (less than QVM2000GFV459) lingual moiety of a right P^3 crown. It consists of the interloph valley and part of the lingual side of the missing main loph. It is significantly larger than *Ngapakaldia bonythoni* P^3 in Black (2010, fig. 2a-a'). The

second specimen NMV P179093, is a crown from the posterior moiety of an M^4 from Top Site. It preserves sufficient features recognised more easily in *Pr. novaculacephalus* M^1 morphology, but in the correct proportion to the regression of form in the QVM2000GFV459 right M^4.

Propalorchestes sp. cf. *P. novaculacephalus*

Referred material. QVM2000GFV406: right dentary fragment, containing M_{2-4} (tables 3–4, figs. 10–12).

Locality and horizon. Bin #25 collected from Top Site, Bullock Creek N.T., Camfield Beds middle Miocene.

Description. The short thick ramus is preserved to a similar extent as the *Pr. novaculacephalus* paratype, NMV P187282: lacks the anterior half of the ventral edge; anterior half of the symphysis; inflected angle; most of the pterygoid fossa; and most of the ascending ramus from a level below the condylar notch. It preserves the following features: a deep semicircular, smoothly concave masseteric fossa with semicircular mandibular masseteric crest that is shallowly concave anteriorly, becoming convex posteriorly in dorsal view; a strong, anteriorly directed coronoid crest on the leading edge of coronoid process level with the anterior root of M_4 in lateral view; a wide intercoronoid sulcus; a small foramen ventral to the interloph valley of M_1 corresponding to the approximate location of the posterior mental foramen of *Propalorchestes* cf *ponticulus,* SGM1008, figured by Murray (1990, fig. 4D); the posterior one third of the symphysis is exposed medially by its fracture; a part of the right genial pit; the M_1 and P_3 alveoli are exposed on buccal side; a dorsomedially directed crest or process on the post-alveolar shelf: and a mandibular foramen on the mid-region of the pterygoid fossa. All cheek teeth are damaged on their lingual side, and the M_2 protoloph is broken at its anterobuccal edge (Figs. 11, 17).

Differs from *Pr. cf ponticulus* AR1779 (Murray, 1990, fig. 4A-C) by its slightly smaller symphyseal dimensions and the genial pit being less ventrally positioned.

Differs from *Pr. cf ponticulus* SGM1008 (Murray, 1990, figs. 4D–F) by having slightly smaller symphysal dimensions, having a slightly larger mandibular ramus and a genial pit that is not as ventrally positioned (tables 3, 4).

Differs from the *Pr. novaculacephalus* paratype NMV P187282 by having a posterior mental foramen that is not paired; having a slightly smaller and more gracile ramus with a depth:width ratio at the M_2 of 1.86 (compared to 2.01 for NMVP187282); the genial pit more ventrally positioned; a M_1 posterior alveolus that is large and not clearly divided; an intercoronoid sulcus that is wide, but less so than in NMV P187282 (89.5 mm width compared to 143.1 mm); dentition not as worn and proportionally broader molars (as wide, but shorter in length) (tables 2–4; figs. 12, 17).

Remarks. QMV2000GFV406 is distinctly smaller than the *Pr. novaculacephalus* paratype NMV P187282; averaging 83.4% of the three mandibular measures and 93.4% of the dentition measures taken for NMVP187282. With respect to the mandibular specimens tentatively referred to *Pr. ponticulus* (Murray, 1990), QMV2000GFV406 is smaller than SGM1008 (averages 86.5%), but has a slightly thicker ramus (104%); it is

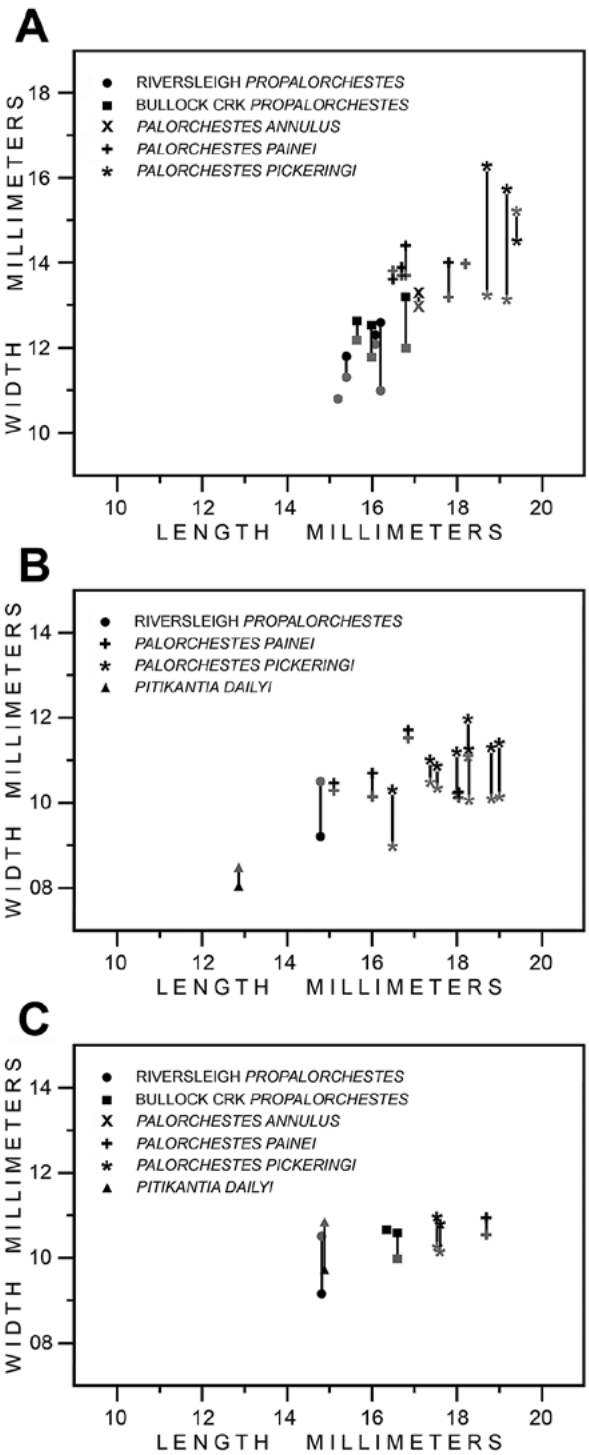

Figure 15. Bivariate plots of dental measures for *Propalorchestes*, small *Palorchestes* and other comparative taxa: a. width against length for M^1; b, width against length for M_1; c, width against length for M_2, to provide comparison with QMV2000GFV406; black symbols represent the anterior loph width and grey symbols represent the posterior loph width; lines connecting black to grey symbols represent the disparity between anterior and posterior measures of the same molar; data and sources provided in Table 1.

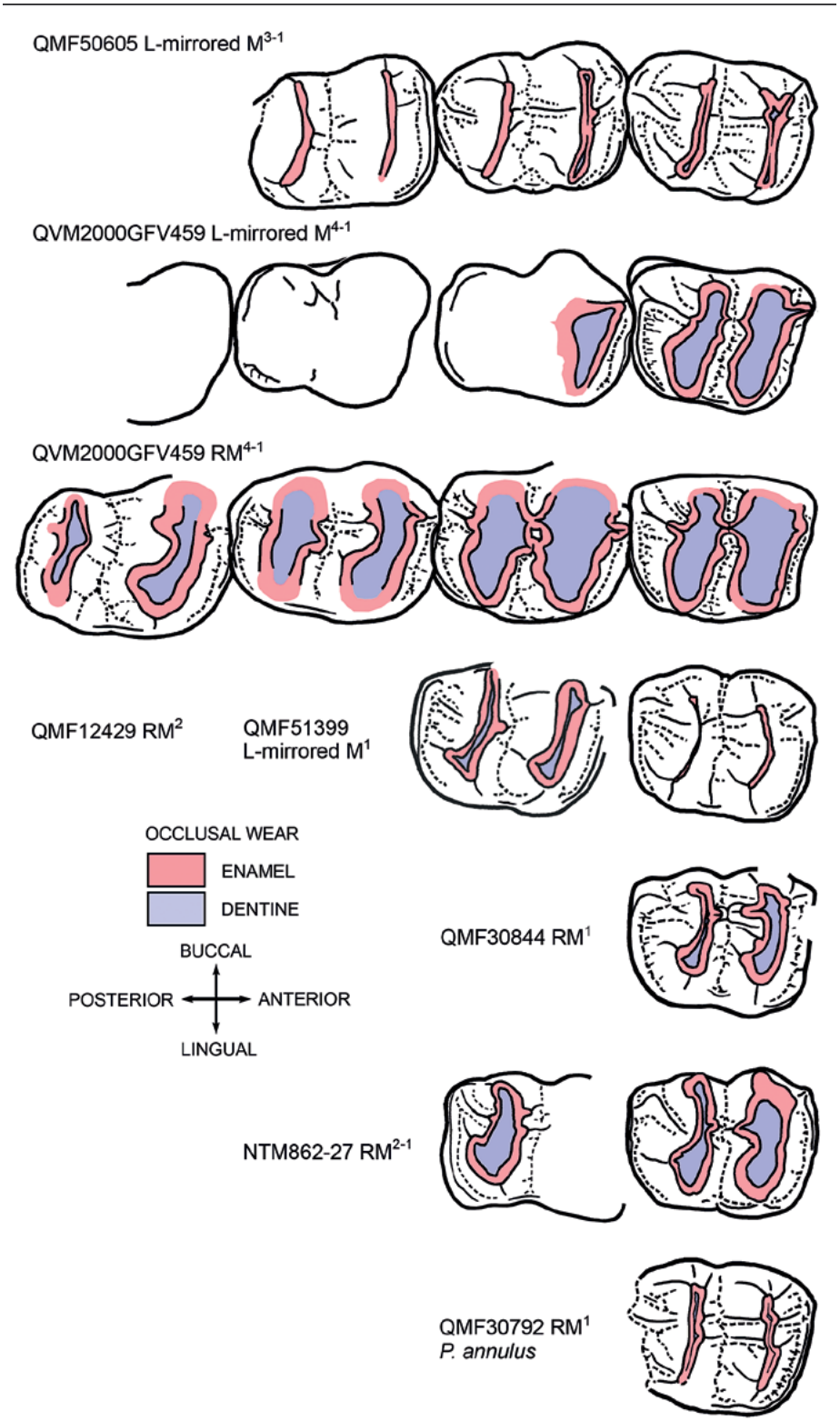

Figure 16. Graphic comparison of QMV2000GFV459 upper molars with previously published *Propalorchetes* material Murray (1990), Black (2006) and *Palorchestes annulus* Black (1997a): specimen outlines scaled so that all M^1 lengths equal that of *Propalorchestes novaculacephalus* NTMP862-27; series depicted from top to bottom in order of increasing M^1 length; left specimens have been reflected for ease of comparison so that the series represents right molars in occlusal view.

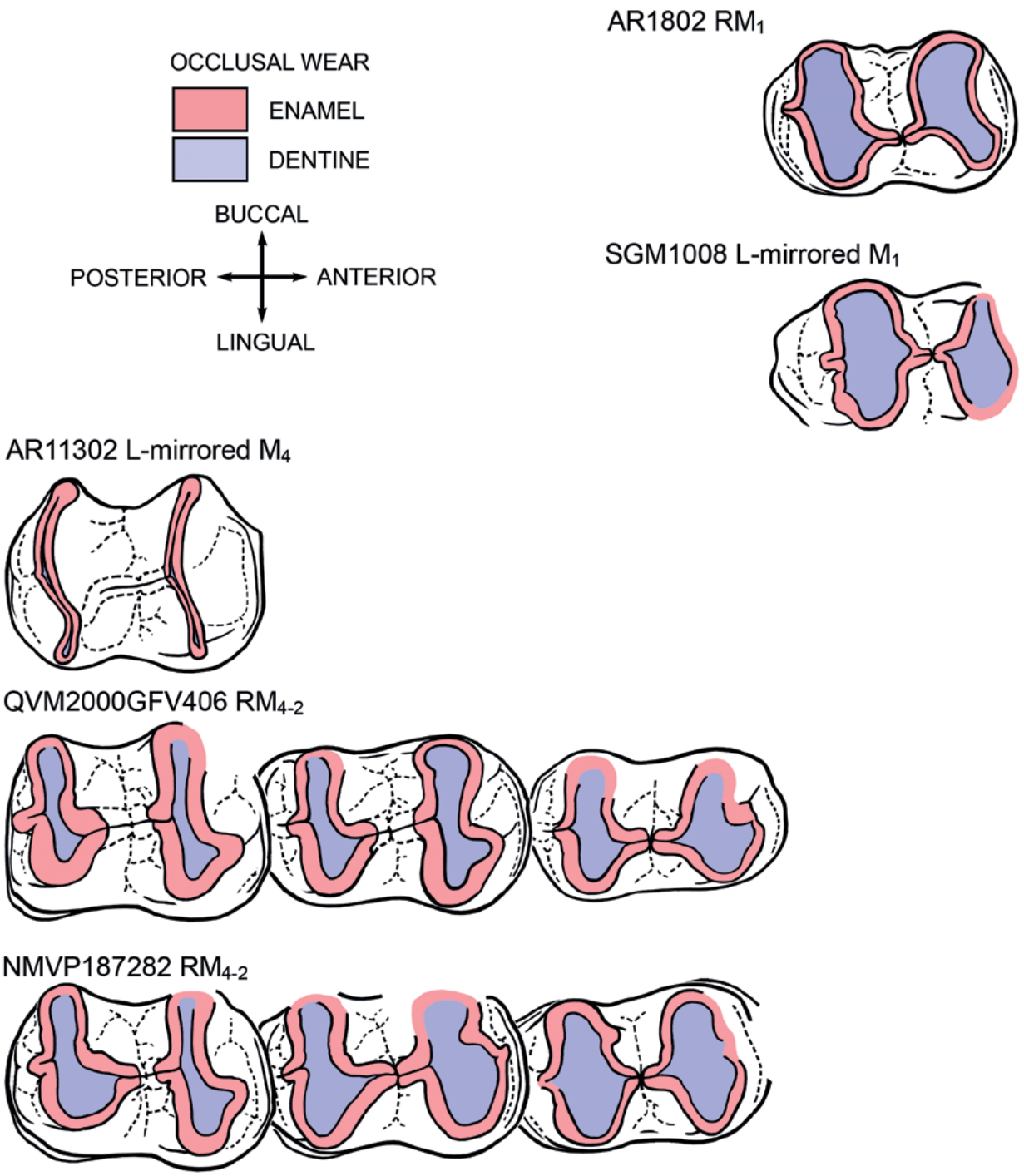

Figure 17. Graphic comparison of QMV2000GFV406 lower right molars in occlusal view with previously published *Propalorchetes* material Murray (1990): M_1 length of QVM2000GFV406 and *Propalorchestes ponticulus* AR1802 Murray (1990) scaled to M_1 of NMVP187282; AR11302 scaled to M_4 of NMVP187282: SGM1008 size approximated to other M_1 material; series depicted top to bottom in order of increasing M_1 length; left specimens have been reflected to become right specimens for ease of comparison.

smaller than AR1779 (86.0% mandibular depth and 95% symphysis width). The location of the genial pit on the posterior surface of the symphysis in QMV2000GFV406 is intermediate between the mid-position it occupies on NMV P187282 and the ventrally positioned pits on the Riversleigh specimens. SMG1008 has the most ventrally located genial pit from the Riversleigh WHA material. Dental measurements for QMV2000GFV406 are also smaller (average 93.75%) than the *Pr. novaculacephalus* paratype NMV P187282 and fractionally larger (average 102% for length) than AR11302 and AR1008 from Riversleigh WHA but 114% wider than AR11302. The QMV2000GFV406 dentition is fractionally larger than that of *Pitikantia dailyi* (tables 2–4; figs. 14, 15).

The general morphology of the new mandible, QMV2000GFV406, is variably comparable to the known *Propalorchestes* material and although smaller than the *Pr. novaculacephalus* NMV P187282 paratype, it is not necessarily more closely aligned to the small Riversleigh WHA Faunal Zones A and B mandibular material tentatively referred to *Pr. ponticulus* (Murray, 1990). As the intercoronoid sulcus of the new specimen is significantly narrower than the *Pr. novaculacephalus* paratype, (this feature is not preserved for *Pr. ponticulus*), and the molar morphology more like Pr. novaculacephalus than *Pr. ponticulus*, it is only tentatively referred to *Pr. novaculacephalus*. Mandibular characters were probably highly variable within populations. For example, when Murray et al. (2000a, b) and Black et al. (2010) described and analysed variation in an extensive number of cranial characters for *Neohelos* and *Nimbadon*, respectively, they demonstrated that mandibular ramus depth and width, and angle of the ascending ramus were subject to both individual, ontogenetic and sexually dimorphic variation.

Dentition. **Lower molars are** roundly rectangular and shallowly waisted at the interlophid valley that is equidistant between the anterior and posterior moieties (figs. 12A, 17). The metalophid and hypolophid are slightly crescentic and curved anteriorly with an expanded protoconid and hypoconid positioned slightly anterobuccally on each loph. The anterior moiety possesses a strong precingulid without a "forelink," but the protoconid is well buttressed anteriorly without connecting to the precingulid. The protoconid is separated from the metaconid by a broad, shallow sulcus that runs to the anterolingual edge of the precingulid cleft. A slight swelling on the precingulid at its midpoint represents a weak paraconid. A moderate "midlink," or cristid obliqua, lies slightly buccal of the crown midline, strongly projecting from the anterior buttressing of the hypoconid and connecting obliquely with a bulge at the base at the midpoint of the posterior face of the metalophid. There is a faint, rounded buccal cingulid. The lingual cingulid is absent. The postcingulid is prominent and connected to the hypolophid by a postlink immediately buccal of the midline. The postlink is clearly delimited on each side by crescentic grooves leading up from the postcingulid valley. Enamel ornament is weaker than on the upper dentition and mostly present on the lingual side of the interlophid valley.

The wear condition of the QVM2000GFV406 dentition is moderate and less extensive than the *Pr. novaculacephalus* NMV P187282 paratype. The morphology of the pre- and postcingulids is less sharply defined.

The apparent morphological progression of the lower molars is as follows: 1. the length gradient increases slightly from M_2-M_4 (QMV2000GFV406 and NMV P187282 do not preserve sufficiently complete lophs for width gradients to be ascertained). 2. the "mid-link" or cristid obliqua is positioned buccal to the midline on M_2 and becomes slightly closer to the midline by M_4. 3. the "mid-link" or cristid obliqua becomes wider from M_2 to M_4. 4. the precingulid becomes less sharply defined from M_2 to M_4. 5. the postcingulid and its shelf becomes less prominent from M_2 to M_4 (figs. 12A, 17).

The $\mathbf{M_1}$ of Pr*opalorchestes ponticulus* has been described in detail by Murray (1990) for the AR1802 holotype and SGM1008. In comparison with the new QVM2000GFV406 mandible and the *Pr. novaculacephalus* paratype NMV P187282, the AR1802 postlink is lingually positioned and contrary to the buccal position to be expected from the tooth progression seen in either mandible. The cristid obliqua is buccally positioned to the degree expected. The morphology that remains on SGM1008 shows hypo- and metalophids proportioned as expected of M_1 on the basis of the dental progression seen in the mandibular tooth rows. The link positions on SGM1008 do not correlate with the progression seen on the mandibular specimens or the *Pr. ponticulus* AR1802 M_1 holotype because the postlink and cristid obliqua are both more medial. Furthermore, AR1802 appears to possess a small double or bisected lingual cingulid.

The $\mathbf{M_2}$ is the smallest and marginally narrowest tooth of the series preserved, but losses and extensive wear, preclude detailed comparisons with the highly worn M_1 morphology of the *Pr. ponticulus* specimens figured by Murray (1990). The postlink and cristid obliqua are narrow and clearly connect with the wear facets.

The $\mathbf{M_3}$ clearly shows that the metaconid is roundly expanded more than the entoconid, but not to the extent of either the hypoconid or larger protoconid. The latter are more triangular in occlusal outline as a result of the anterior extensions produced by the connection of the cristid obliqua to the hypoconid, and the anterior buttressing of the protoconid.

$\mathbf{M_4}$ is the largest tooth showing a broader morphology of the cristid obliqua, postlink and cingulids; the buccal cingulid is scarcely evident. The metaconid is least expanded and subequal with the entoconid. The cristid obliqua and postlink are close to the longitudinal midline. The referred *Pr. ponticulus* AR11302 was described by Murray (1990) as a possibly encrypted, but isolated M_4. It exhibits a closer morphology to the M_4s of QVM2000GFV406 and the *Pr. novaculacephalus* paratype NMV P187282 (figs. 12A, B, 17).

Discussion

The morphology and extent of retraction of the nasal anatomy seen in the QVM2000GFV459 specimen is comparable with the degree of retraction seen in *P. painei* from the Miocene, *P. parvus* from the Pliocene to Pleistocene and the last surviving palorchestid species, *P. azael* from the late Pleistocene (fig. 9). Minor details of the morphology vary between each, indicating that *Palorchestes* continued to develop specialisations of the

rostrum in addition to the allometric changes related to evolving larger skull and body size. Detailed morphometric analyses are presently beyond the scope of this description, but with the relative completeness of cranial material now available from *Pr. novaculacephalus*, *P. painei,* and *P. azael*, a more precise relationship between allometry, morphological function and phylogenetic trends might be elucidated.

The vertical elaboration of the face and rostrum of palorchestid skulls represented in chronological sequence, indicates a relationship to an allometry that may be independent of the primary nasal function. For example, the retracted condition of the nasals and dorsal exposure of the nasal cavity to a level immediately anterior to the orientation of the transverse facial plane in *P. painei* had already been achieved in *Propalorchestes*. Furthermore, the morphology is very close to the aligned condition of the facial plane, the proximal limit of the nasal aperture, and the orbits found in *P. azael*. (figs. 3, 5, 6, 9). The progression of increasing vertical height of the skull and face in *Palorchestes* occurred while maintaining the close relationship between the proximal limit to which the nasal was retracted, the transverse facial plane, and the orbits that are now known to have been present in *Propalorchestes.*

The relative projection of the rostrum from the transverse facial plane and the deflexion of the rostrum from the frontal plane (measured against the horizontal tooth row) also increased from *Propalorchestes* to the largest *Palorchestes.* The proportional changes indicate that as the height of the skull increased, the orbits and retracted nasals were taken with it and together, their relative position continued to move posteriorly. In *Propalorchestes* the retracted nasals are aligned with the P^3. In *Palorchestes painei* the alignment had moved slightly to a point between P^3 and M^1, while in *P. azael,* they align with the posterior moiety of M^3 (fig. 9). In relative terms, the food procuring and processing anatomy has projected anteriorly with respect to the eyes and nasal cavity. The nasals have not retracted posterior to the eyes in *P. azael,* nor have the orbits maintained their position relative to the tooth row. Allometry and masticatory function may both be influencing the rostrum morphology in this context. Testing the complex factors in this morphological progression for the Palorchestidae will likely remain elusive and would be pivotal on a more complete knowledge of the cranial form of later, more advanced small palorchestids such as *P. pickeringi*. Due to the apomorphic rostral condition now revealed in *Propalorchestes*, understanding the factors surrounding its origin will require a more archaic member of the family; one representing a truly intermediate condition, (e.g. intermediate between the rostral form of genera such as *Ngapakaldia,* Diprotodontinae and that of *Propalorchestes novaculacephalus*).

Extensive descriptions of individual *Propalorchestes* teeth have been given in the literature (Murray, 1990; Mackness, 1995; Black, 1997a, 2006). Black (2006) remarked that poor preservation and heavy occlusal wear precluded many character comparisons and creates sparse measurement opportunities for meaningful comparisons. The extreme individual variation in dental morphology within extinct Vombatiformes is well known (Black, 2006; Price and Sobbe, 2010). Without a substantial data set, variation within any given population between geographical regions, or over substantial periods of time, is difficult to define for fossil taxa. Regarding extant Vombatiformes, Black et al. (2014) detailed modern koala dental variation and related it to fossil taxa. Sharp and Trusler (2015) provide a brief summary of the morphological variation seen in the wombat genera *Vombatus* and *Lasiorhinus.* Following re-examination of Riversleigh *Propalorchestes,* Black (2006) reassigned two *Pr. ponticulus* upper molar specimens, previously described from Faunal Zone B deposits (Black, 1997a, b), to *Pr. novaculacephalus* following study of a new juvenile maxilla fragment with well preserved unworn teeth from a Faunal Zone C deposit. Black (2006) concluded that *Propalorchestes* range throughout Faunal Zones A–C exhibiting a morphocline with the more plesiomorphic forms in the oldest Faunal Zone A deposits, but essentially places two forms, for which species boundaries are continuing to be redefined, at opposing ends of the late Oligocene to middle Miocene interval. Further evidence of this trend has been presented by Arena et al. (2015) with the inclusion of upper dentition attributed to *Propalorchestes ponticulus,* that until this time had only been represented by lower dentition. *Propalorchestes novaculacephalus* is represented by upper and lower dentition from the Bullock Creek LF, but only by upper dentition from Riversleigh Faunal Zone B and C deposits. The diagnosis upon which this had largely depended was based upon NMV P187282, an isolated dentary fragment with $M_{2\text{-}4}$ and NTMP862-27, a partial maxilla from Bullock Creek bearing incomplete crowns $M^{2\text{-}3}$ (Murray, 1990). Unfortunately, the new material contained in the biochronostratigraphic study of Arena et al. (2015:10) was provided without supporting information, stating that "*Propalorchestes* molars are usually heavily worn. Consequently, molar size and shape are the most useful features for differentiating between species."

Issues concerning the relative states of morphological progression are a major part of the dental literature for palorchestids. For example, Black (2006: 356) stated with respect to the interloph cristae that, "This structure may represent a precursor to a true 'midlink'…these cristae and enamel bulges do not constitute the true midlink, a synapomorphy that unites species of *Palorchestes* (Mackness 1995) to the exclusion of species of *Propalorchestes*." Murray (1990: 41) described NTMP862-27 as "possessing 'a double midlink-like structure' formed on either side of a rhomboidal fossa that is positioned buccal of the midline in the interloph valley."

The difference between cristae and links is a matter of degree, both in terms of evolutionary trends within a population over time and the morphological progression within the dental series, consequent of the ontogenetic inhibitory cascade expression in any individual (Kavanagh et al., 2007; Halliday and Goswami, 2013). The condition and relative wear of the dentition also alters the perception of the morphology and it is clearly seen to influence the descriptions and interpretation of the same features. Like NTMP682-27, both M^1s on QVM2000GFV459 possess a bulge at the midline of the anterior face of the metaloph. This is recorded as a lobe on the wear facet occlusal outline. The Riversleigh WHA *Pr. novaculacephalus* M^1s possess incipient bulges (to varying

extents) in the same location, but the lesser wear on these specimens precludes strong indication of their bulging form on the occlusal facet outline. Examination of the dentition in all *Palorchestes* species through a complete range of wear reveals that the bulges, cristae and links are essentially folds of enamel and seldom appear to be fused. This is particularly the case with the midlinks where a highly worn state will produce a characteristic cross in occlusal outline. This is attained when the entire length of the midlink makes occlusal contact and the transverse line (fine cleft) of the cross persists until the ware has entirely breached the enamel. The same pattern and process occurs with the enamel constituting the buccal and lingual sides of the midlink, with the division between them persisting as the sagittal line of the cross until the enamel is breached. The enamel links are just tightly abutted (fig. 13). The morphological expression is one of degree and neither a union or a failure to have reached a union, strictly speaking, occurs as a character state. Swellings on the posterolingual faces of the protocone and metaconule also form buttresses that accentuate the recurvature of the crescentic lophs as occlusal wear advances. These are variably developed and also become cristae in the more derived *Palorchestes.*

With regard to the evolutionary development of links between cusps or lophs, the *Pr. novaculacephalus* paratype QMF12429 exhibits misaligned bulges or incipient cristae in the interloph valley. The topographic growth of aligned features by height, length or duplication would easily allow progression to be determined from primitive to advanced states. If major realignments are required to form a connection between features (i.e. to establish a midlink in a derived morphology) the path of development from an unknown origin will be more difficult to determine. Such variability in character states makes it difficult to reconcile the different emphases placed upon them by Murray (1990) and Black (2006) to that of our own. In reviewing *Pr. novaculacephalus,* Black (2006: 358) concluded "differences between the referred specimens and the paratypes do not warrant specific distinction." The QMF12429 paratype does not appear to fit within the stated evolutionary trend for the most significant taxonomic character of the palorchestid dentition. The spectrum of variation in the other *Propalorchestes* material and of the new material described here falls closer to a transitional progression towards the development of a midlink and indeed, a double midlink in *Palorchestes,* irrespective of where one might delimit taxonomic boundaries. At worst, QMF12429 may simply be aberrant, and at best, may indicate a deviation from the assumed lineage for which it was designated as a paratype.

Similar trends are evident in the lower cheek teeth. The extent that such morphologies become confluent with the tips of the cusps and loph ridges of the crown is always going to be increasingly indeterminable with advancing wear. This makes character conditions difficult to define in a majority of specimens. The definition of fore- and postlinks is less problematic in this respect because the wear is generally less extensive across the more basal regions of the crown and a complete bridge of the form in question with the pre- and postcingulae more easily determined.

Inconsistencies between the *Pr. ponticulus* published material leads us to reiterate the uncertainties originally stated when the material was described and additional material referred to the taxon. Despite the size discrepancy between the mandibles recovered from the Bullock Creek sites, the dentition is similar and shows a consistent morphological relationship. The morphological similarity between the AR11302 M_4, QVM2000GFV406 and the *Pr. novaculacephalus* holotype M_4s is strong. It is more consistent than the M_1 *Pr. ponticulus* material from the Riversleigh WHA exhibits between them or would be suggested from the molar morphological progression seen in the mandibular specimens from Bullock Creek. This leads us to tentatively refer AR11302 to *Propalorchestes novaculacephalus* as the first lower dentition of the species from the Riversleigh Wayne's Wok Locality, Faunal Zone B (Archer et al., 1989). This would be consistent with Black (2006) who stated that *Pr. novaculacephalus* (upper dentition) is first recorded in FZ B deposits and becomes more common in the later FZ C, and independently agrees with Arena et al. (2015)

Colbert (2006) regarded the common practice of referring isolated tapiroid dental material to a particular genus or higher taxon without cranial evidence as problematic and a similar issue becomes evident here. The degree of plesiomorphy in the dentition belies the specialization of the facial morphology in *Propalorchestes.* At the outset, Murray (1986: 209) noted a mosaic of characters in the neurocranial fragment of the holotype, concluding "*Propalorchestes* is generally more primitive and simultaneously more specialized than *Palorchestes*." He was referring to the only near-complete skulls of the genus available, those of *P. painei.* Despite this astute observation, taxonomic deliberations have proceeded–inevitably concentrating on isolated teeth. Three studies have added to, and sought to resolve the Oligo-Miocne palorchestid material from the Riversleigh WHA since Murray (1990) first erected *Pr. ponticulus* (Black 1997a, 2006; Arena et al., 2015*).* The known issues of dental variation in fossil herbivorous marsupial species (Murray et al., 2000a; Black and Hand, 2010; Black et al., 2013) apply well to *Propalorchestes*, testing the assumption that meaningful taxonomic boundaries can be applied to encapsulate apparent trends in small samples.

Conclusion

Together with the two fragmentary maxillae and single basicranial holotype specimen, the analysis of this important new cranial material provides the most complete reconstruction of skull morphology in Palorchestidae to date. *Propalorchestes* confirms the presence of the *Palorchestes*-like retracted nasal and rostral anatomy for an otherwise smaller, early and dentally plesiomorphic member of the family. Furthermore, it reveals the advanced stage of evolution of the specialized retracted nasal structure attained within the lineage by the early to middle Miocene, and at a time when trends to larger and disparately specialized lineages were only just beginning to indicate the magnitude of rostral morphological divergence that zygomaturines and diprotodontines would attain by the Pleistocene (Murray, 1992). Together with further studies of

more complete cranial material of *Palorchestes azael* from the late Pleistocene (study presently underway), the evolutionary patterns within the family may become better understood (despite the comparative rarity of palorchestids in the fossil record). The advanced state of the elongated and exposed nasal anatomy in *Propalorchestes* indicates that the unique palorchestid splanchnocranium, its function, and the niche in which it was employed, was present by the middle Miocene and may have a significant earlier history.

Acknowledgements

Many people have contributed to the collection, preparation and CT scanning of the specimens described in this paper. We would like to thank the expedition members present at Bullock Creek when the specimens were collected (in alphabetical order; Michael Archer, Christoph Balouet, Frank Bussat, Georgie Clayton, Tim Flannery, Sue Hand, Cindy Hann, Faye Ovendon, Rosendo Pasqual Thomas Rich, Betty Thompson, Hans van Vlodrop, Patricia Vickers-Rich; the Camfield Station owner at that time, Mrs Enid Dayes, manager, Baden Black, cartage contractors, Tom Byrnes, Transport, Katharine; Dr Erich Fitzgerald for alerting us to the unidentified skull and for the opportunity to prepare this paper; Craig McCormack and Laurie Austen, preparators at the QVMAG, for their judicious skill in revealing the specimens for study; Craig Reid, Collection Officer at the Queen Victoria Museum and Art Gallery for providing access to the material and study facilities; Garth Faulkner, Chief Radiographer/Manager, and Mathew Limbrick, Senior CT Specialist, from the Department of Medical Imaging, Launceston General Hospital for scanning the specimens; additional collections access provided by Dr Scott Hocknull and Kristen Spring, Geosciences Collections, Queensland Museum, Hendra; David Pickering and Dr Thomas Rich, Palaeontology, Museum Victoria, Carlton Gardens; and Dr Neville Pledge and Mary-Anne Binnie, Palaeontology, South Australian Museum, Adelaide. Funding for this study has been provided through the Central Scholarship system at Monash University for the doctoral studies of both authors. Our appreciation for the personal assistance given during the manuscript preparation by Sally Simpson, Gael Trusler and Oliver Trusler.

We are greatly indebted to the reviewers and editor for their thoughtful and constructive comments.

References

Aplin, K.P., and Archer, M. 1987. Recent advances in marsupial systematics with a new syncretic classification. In *Possums and Opossums: Studies in evolution*. Ed M. Archer: xv-lxxii. Beatty and Sons and the Zoological Society of New South Wales: Sydney.

Archer, M., and Bartholomai, A. 1978. Tertiary mammals of Australia: a synoptic review. *Alcheringa*, 2: 1-19.

Archer, M., Hand, S.J., & Godthelp, H. 1991. *Riversleigh: The Story of Animals in Ancient Rainforests of Inland Australia*. Reed Books, Sydney, 264 pp.

Archer, M., Godthelp, H., Hand, S., and Megirian, D. 1989. Fossil mammals of Riversleigh, northwestern Queensland: preliminary overview of biostratigraphy, correlation and environmental change. *Australian Zoologist* 25(2): 29-65.

Archer, M., Hand, S.J., Godthelp, H., and Creaser, P. 1997. Correlation of the Cainozoic sediments of the Riversleigh World Heritage Fossil Property, Queensland, Australia. In: J.-P. Aguilar, S. Legendre, and J. Michaux (eds.), *Actes du Congres BiocroM'97*, 131-152. Memoirs et Traveaux Ecole Pratique des Hautes Etudes, Institut de Montpellier, Montpellier.

Archer, M., Arena, D.A., Bassarova, M., Beck, R.M.D., Black, K., Boles, W.E., Brewer, P., Cooke, B.N., Crosby, K., Gillespie, A., Godthelp, H., Hand, S.J., Kear, B.P., Louys, J., Morrell, A., Muirhead, J., Roberts, K.K., Scanlon, J.D., Travouillon, K.J., and Wroe, S. 2006. Current status of species-level representation in faunas from selected fossil localities in the Riversleigh World Heritage Area, northwestern Queensland. *Alcheringa* 30(2 supp 1): 1-17.

Arena, D.A. 2004. *The Geological History and Development of the Terrain at the Riversleigh World Heritage Area during the Middle Tertiary*, 275 pp. Unpublished Ph.D. Thesis, University of New South Wales, Sydney.

Arena, D.A., Travouillon, K.J., Beck, R.M.D., Black, K.H., Gillespie, A.K., Myers, T.J., Archer, M., & Hand, S.J. 2015. Mammalian lineages and the biostratigraphy and biochronology of Cenozoic faunas from the Riversleigh World Heritage Area, Australia. *Lethaia*, DOI: 10.1111/let.12131.

Black, K.H. 1997a. A new species of Palorchestidae (Marsupialia) from the late middle to early late Miocene Encore Local Fauna, Riversleigh, northwestern Queensland. *Memoirs of the Queensland Museum* 41: 181-5.

Black, K.H. 1997b. Diversity and biostratigraphy o f the Diprotodontoidea of Riversleigh, northwestern Queensland. *Memoirs of the Queensland Museum* 41: 187-92.

Black, K.H. 2006. Description of new material for *Propalorchestes novaculacephalus* (Marsupialia: Palorchestidae) from the mid Miocene of Riversleigh, northwestern Queensland. *Alcheringa* 30(2): 351–361.

Black, K.H. 2010. *Ngapakaldia bonythoni* (Marsupialia, Diprotodntidae): new material from Riversleigh, northwestern Queensland, and a reassessment of the genus *Bematherium*. *Alcheringa*, 34(4): 471–492.

Black, K.H., Archer, M., Hand, S. J., and Godthelp, H. 2010. First comprehensive analysis of the cranial ontogeny in a fossil marsupial - from a 15-million-year-old cave deposit in northern Australia. Journal of Vertebrate Paleontology, 30: 993-1011.

Black, K.H., Archer, M., Hand, S J., and Godthelp, H. 2012. The Rise of Australian Marsupials: A Synopsis of Biostratigraphic, Phylogenetic, Palaeoecologic and Palaeobiogeographic Understanding. In J.A. Talent (ed.) 2012, *Earth and Life, International Year of Planet Earth,* 983-1078. Springer Science+Business Media B.V. DOI 10.1007/978-90-481-3428-1_35.

Black, K.H., Archer, M., Hand, S.J., and Godthelp, H. 2013. Revision in the marsupial diprotodontid genus *Neohelos*: systematics and biostratigraphy. *Acta Palaeontologica Polonica* 58, 679–706.

Black, K.H., and Hand, S.J. 2010. First crania and assessment of species boundaries in Nimbadon (Marsupialia: Diprotodontidae) from the middle Miocene of Australia. *American Museum Novitates* 3678: 1-60. http://dx.doi.org/10.1206/666.1.

Black, K.H., Louys, J., and Price, G.J. 2014. Understanding morphological variation in the extant Koala as a framework for identification of species boundaries in extinct Koalas (Phascolarctidae: Marsupialia). *Journal of Systematic Palaeontology* 12(2):237-264.DOI:10.1080/14772019.2013.768304.

Black, K.H., and Mackness, B. 1999. Diversity and relationships of diprotodontoid marsupials. *Australian Mammalogy* 21: 20-21, 34-45.

Boas, J.E.V., and Paulli, S. 1908. *The elephant's head; Studies in the comparative anatomy of the origins of the head of the Indian Elephant and other mammals.* Part 1. The facial muscles and the proboscis. Carlsberg-Fund, Copenhagen.

Boas, J.E.V., and Paulli, S. 1924. *The elephant's head; Studies in the comparative anatomy of the origins of the head of the Indian Elephant and other mammals.* Part 2. Carlsberg-Fund, Copenhagen.

Colbert, M.W. 2006. *Hesperaletes* (Mammalia: Perissodactyla), a new tapiroid from the Middle Eocene of southern California. *Journal of Vertebrate Paleontology*, 26(3): 697-711.

Flannery, T.F., Archer, M., and Plane, M. 1982. Middle Miocene kangaroos (Macropodoidea, Marsupialia) from 3 localities in northern Australia, with a description of 2 new subfamilies. *BMR Journal of Australian Geology & Geophysics,* 7(4), 287-302.

Gillespie, A.K., Archer, M., Hand, S.J., and Black, K.H. 2014. New material referable to *Wakaleo* (Marsupialia: Thylacoleonidae) from the Riversleigh World Heritage Area, northwestern Queensland: Revising species boundaries and distributions in Oligo/Miocene marsupial lions. *Alcheringa*, 38(4): 513-527. DOI: 10.1080/03115518.2014.908268.

Halliday, T.J.D., and Goswami, A. 2013. Testing the inhibitory cascade model in Mesozoic and Cenozoic mammaliaforms. *BMC Evolutionary Biology,* 13: 79 doi:10.1186/1471-2148-13-79.

Kavanagh, K.D., Evans, A.R. and Jernvall, J. 2007. Predicting evolutionary patterns of mammalian teeth from development. Nature, 449: 427-433. doi:10.1038/nature06153.

Illiger, C. 1811. *Prodromus systematis mammalium et avium additus termminus zoographicus utridque classis*. Berlin, C.Salfeld.

Luckett, W.P. 1993. An ontogenetic assessment of dental homologies in therian mammals. In: F.S. Szalay, M.J. Novacek, and M.C. McKenna (eds.), *Mammal Phylogeny: Mesozoic differentiation, multituberculates, monotremes, early therians and marsupials*, 182-204. Springer-Verlag, New York, New York.

Mackness, B. 1995. *Palorchestes selestiae*, a new species of palorchestid marsupial from the Early Pliocene Bluff Downs local fauna, northeastern Queensland. *Memoirs of the Queensland Museum* 38: 603-609.

Mackness, B. S. 2008. Reconstructing *Palorchestes* (Marsupialia: Palorchestidae) – from giant kangaroo to marsupial 'tapir'. *Proceedings of the Linnean Society of New South Wales*, 130: 21-36.

McGowran, B. and Li, Q. 1994. The Miocene oscillation in southern Australia. *In:* Pledge N. S. ed. *Australian Vertebrate Evolution, Palaeontology and Systematics*, pp. 197–212. *Records of the South Australian Museum*, 27: 197–212.

Megirian, D. 1994. Approaches to marsupial biochronology in Australia and New Guinea. *Alcheringa* 18(3): 259–274.

Megirian, D., 1997. *The geology of the Carl Creek Limestone, northwestern Queensland*. Unpublished PhD thesis, Flinders University, Adelaide, 530 pp. + appendices 1-5.

Megirian, D., Murray, P., Schwartz, L., and Von Der Borch, C. 2004. Late Oligocene Kangaroo Well Local Fauna from the Ulta Limestone (new name), and climate of the Miocene oscillation across central Australia. *Australian Journal of Earth Sciences,* 51 (5): 701-741.

Megirian, D., Prideaux, G.J., Murray, P.F., and Smit, N. 2010. An Australian land mammal age biochronological scheme. *Paleobiology* 36(4): 658-671. http://dx.doi.org/10.1666/09047.1.

Murray, P.F. 1986. *Propalorchestes novaculacephalus* gen et sp. nov., a new palorchestid (Marsupialia: Palorchestidae) from the mid Miocene Camfield Beds, Northern Territory Australia. *The Beagle, Records of the Northern Territory Museum of Arts and Sciences* 3(1): 195–211.

Murray, P.F. 1990. Primitive marsupial tapirs (*Propalorchestes novaculacephalus* Murray and *Propalorchestes ponticulus* sp. nov.) from the mid Miocene of North Australia. (Marsupialia: Palorchestidae) *The Beagle, Records of the Northern Territory Museum of Arts and Sciences* 7(2): 39–51.

Murray, P.F. 1992 Thinheads, thickheads and airheads – Functional craniology of some diprotodontian marsupials. *The Beagle, Records of the Northern Territory Museum of Arts and Sciences* 9(1): 71-88.

Murray, P.F., and Megirian, D. 1992. Continuity and contrast in Middle and Late Miocene vertebrate communities from the Northern Territory. *The Beagle, Records of the Northern Territory Museum of Arts and Sciences* 9(1): 195-218.

Murray, P.F., Megirian, D., Rich, T., Plane, M., Black, K.H., Archer, M., Hand, S.J., and Vickers-Rich, P. 2000a. Morphology, Systematics, and Evolution of the Marsupial Genus *Neohelos* Stirton (Diprotodontidae, Zygomaturinae). *Museums and Art Galleries of the Northern Territory Research Report No. 6*: 1-141.

Murray, P.F., Megirian, D., Rich, T.H., Plane, M., and Vickers-Rich, P. 2000b. *Neohelos stirtoni*, a new species of Zygomaturinae (Diprotodontidae: Marsupialia) from the mid-Tertiary of northern Australia. *Memoirs of the Queen Victoria Museum* 105: 1-47.

Murray, P.F., and Vickers-Rich, P. 2003, *"Magnificent Mihirungs"*, Indiana University Press, Bloomington.

Myers, T. J., Archer, M. 1997. *Kuterintja ngama* (Marsupialia, Ilariidae): a revised systematic analysis based on material from the late Oligocene of Riversleigh, northwestern Queensland. *Memoirs of the Queensland Museum* 41, 379–392.

Owen, R. 1866. *On the anatomy of vertebrates,* Vol. II. Longmans, Green, London.

Piper, K.J. 2006. A new species of Palorchestidae (Marsupalia) from the Pliocene and Early Pleistocene of Victoria. *Alcheringa*, Special Issue 1: 281-294.

Plane, M.D., and Gatehouse, C. 1968. A new vertebrate fauna from the Tertiary of Northern Australia. *Australian Journal of Science* 30: 271-273.

Pledge, N.S. 1991. Occurances of *Palorchestes* species (Marsupialia: Palorchestidae) in South Australia. *Records of the South Australian Museum* 25(2): 161-174.

Pledge, N.S. 1992. Curramulka Local Fauna: a Late Tertiary fossil assemblage from Yorke Peninsula, South Australia. *The Beagle, Records of the Northern Territory Museum of Arts and Sciences* 9: 115-142.

Price, G.J., and Hocknull, S.A. 2005. A small adult *Palorcherstes* (Marsupialia, Palorchestididae) from the Pleistocene of Darling Downs, southeastern Queensland. *Memoirs of the Queensland Museum* 51(1): 202.

Price, G.J., and Sobbe, I.H. 2010. Morphological variation within an individual Pleistocene Diprotodon optatum Owen, 1838 (Diprotodontinae; Marsupialia): implications for taxonomy within diprotodontoids. *Alcheringa: An Australasian Journal of Palaeontology* 35(1): 21-29. http://dx.doi.org/10.1080/03115511003793553.

Randal, M.A., and Brown, M.C. 1967. The geology of the northern part of the Wiso Basin. *Bureau of Mineral Resources, Geology and Geophysics, Australia, Record* 11:10.

Rich, T.H. 1991. Monotremes, placentals, and marsupials: their record in Australia and its biases. In *Vertebrate Palaeontology of Australasia*, P. Vickers-Rich, J.M. Monaghan, R.F. Baird & T.H. Rich eds, Pioneer Design Studio and Monash University Publications Committee, Melbourne, 893-1070.

Rich, T.H., and Archer, M. 1979. *Namilamadeta snideri,* a new diprotodontan (Marsupialia, Vombatoidea) from the medial Miocene of South Australia. *Alcheringa* 3: 197-208.

Sharp, A.C. (2016) A quantitative comparative analysis of the size of the frontoparietal sinuses and brain in vombatiform marsupials. *Memoirs of Museum Victoria* 74: 331–342

Sharp, A.C., and Trusler, P.W. 2015. Morphology of the jaw-closing musculature in the Common Wombat (*Vombatus ursinus*) using digital dissection and magnetic resonance imaging. *PLoS ONE* 10(2): e0117730. doi:10.1371/journal.pone.0117730.

Shean, D.A. 2007. *Geochronology, taxonomy and morphology of select fossils of the Buchan Caves, South-eastern Australia*. Masters qualifying thesis, Monash University, Clayton, Victoria, Unpublished.

Smith, M.J., and Plane, M. 1985. Pythonine snakes (Boidae) from the Miocene of Australia. *BMR Journal of Australian Geology and Geophysics,* 9: 191-195.

Stirton, R. 1967. The Diprotodontidae from the Ngapakaldi Fauna, South Australia. In: R. Stirton, M. Woodburne and M. Plane (eds.) *Tertiary Diprotodomidae from Australia and New Guinea. Bureau o f Mineral Resources Geology and Geophysics Bulletin* 85: 3-35.

Stirton, R., Woodburne, M., and Plane, M. 1967. A phylogeny of the Tertiary Diprotodontidae and its significance in correlation. In: R. Stirton, M. Woodburne, and M. Plane (eds.), *Bureau of Mineral Resources, Geology and Geophysics, Australia, Bulletin* 85: 45-51.

Stirton, R.A., Tedford, R.H., & Woodburne, M.O. 1968. Australian Tertiary deposits containing terrestrial mammals. *University of California Publications in Geological Sciences 77*: 1-30.

Tate, G. H. H. 1948. Studies on the anatomy and phylogeny of the Macropodidae (Marsupialia). Results of the Archbold Expedition, No 59. *Bulletin of the American Museum of Natural History*, 91(2): 237-351.

Tedford, R. 1966. Fossil mammal remains from the Tertiary Carl Creek Limestone, north-western Queensland. *Bureau of Mineral Resources Geology and Geophysics Bulletin* 92: 217-237.

Travouillon, K.J., Archer, M., Hand, S.J., and Godthelp, H. 2006. Multivariate analyses of Cenozoic mammalian faunas from Riversleigh, northwestern Queensland. *Alcheringa*, Special Issue 1, 323–349.

Travouillon, K.J., Legendre, S., Archer, M., and Hand, S.J. 2009. Palaeoecological analyses of Riversleigh's Oligo-Miocene sites: Implications for Oligo-Miocene climate change in Australia. *Palaeogeography, Palaeoclimatology, Palaeoecology,* 276 (1): 24-37.

Witmer, L.M., Sampson, S.D., and Solunias, N. 1999. The proboscis of tapirs (Mammalia: Perissodactyla): a case study in novel narial anatomy. *Journal of Zoology (London)* 249: 249-267.

Woodburne, M.O. 1967b. The Alcoota fauna, Central Australia. An integrated palaeontological and geological study. *Bulletin of the Bureau of Mineral Rescources* 87: 1-178.

Woodburne, M.O. 1984. Families of marsupials: relationships, evolution and biogeography. In Mammals: Notes for a Short Course, T.W. Broad-Head, ed., *University of Tennessee Department of Geological Sciences, Studies in Geology*, 8: 48–71.

Woodburne, M.O., MacFadden, B.J., Case, J.A., Springer, M.S., Pledge, N.S., Power, J.D., Woodburne, J.M., and Springer, K.B. 1994. Land mammal biostratigraphy and magnetostratigraphy of the Etadunna Formation (late Oligocene) of South Australia. *Journal of Vertebrate Paleontology* 13(4): 483-515. http://dx.doi.org/10.1080/02724634.1994.10011527

Woodburne, M.O., Tedford, R.H., Archer, M., Turnbull, W.D., Plane, M.D., and Lundelius, E.L. 1985. Biochronology of the continental mammal record of Australia and New Guinea. In *Stratigraphy, Palaeontology, Malacology: Papers in Honour of* Dr Nell Ludbrook, J.M. Lindsay ed., *Special Publication of the South Australian Department of Mines and Energy* 5: 347-363.

Woodhead, J., Hand, S.J., Archer , M., Graham, I., Sniderman , K., Arena, D. A., Black, K.H., Godthelp, H., Creaser, P., and Price, E. 2015. Developing a radiometrically-dated chronologic sequence for Neogene biotic change in Australia, from the Riversleigh World Heritage Area of Queensland. *Gondwana Research*, http://dx.doi.org/10.1016/j.gr.2014.10.004.

Woods, J. T. 1958. The extinct marsupial genus *Palorchestes* Owen. *Memoirs of the Queensland Museum,* 13: 177-193.

Wroe, S., Brammall, J., and Cooke, B. N. 1998. The skull of *Ekeltadeta ima* (Marsupialia, Hypsipyrmnodontidae?): An analysis of some marsupial cranial features and a re-investigation of Propleopine phylogeny, with notes on the inference of carnivory in mammals. *Journal of Paleontology*, 72(4): 738-751.

Online supplementary material

Table S1. Upper cheek teeth measurements for *Propalorchestes*, smaller *Palorchestes* species and other comparative taxa discussed throughout this study (mm).

Table S2. Lower cheek teeth measurements for *Propalorchestes*, smaller *Palorchestes* species and other comparative taxa discussed throughout this study (mm).

FIGURE S1. 3-D interactive pdf of QVM2000GFV459 paratype ; opaque and transparent options to show endocranial sinuses in blue and endocranial cavity in red.